Distribution Category:
Defense Waste Management
(UC-721)

ANL-95/21

ARGONNE NATIONAL LABORATORY
9700 South Cass Avenue
Argonne, IL 60439

VALIDATION OF THE GENERIC TRUEX MODEL USING DATA FROM TRUEX DEMONSTRATIONS WITH ACTUAL HIGH-LEVEL WASTE

by

M. C. Regalbuto, S. Aase, and G. F. Vandegrift
Chemical Technology Division

DISCLAIMER

DISCLAIMER

Portions of this document may be illegible in electronic image products. Images are produced from the best available original document.

TABLE OF CONTENTS

LIST OF FIGURES

LIST OF FIGURES (contd)

LIST OF FIGURES (contd)

LIST OF FIGURES (contd)

LIST OF FIGURES (contd)

LIST OF TABLES

VALIDATION OF THE GENERIC TRUEX MODEL USING DATA FROM TRUEX DEMONSTRATIONS WITH ACTUAL HIGH-LEVEL WASTE

by

M. C. Regalbuto, S. Aase, and G. F. Vandegrift

ABSTRACT

The Generic TRUEX Model (GTM) was used to simulate three different countercurrent flowsheet tests performed using mixer-settlers that had been carried out prior to 1993 in the Chemical Processing Facility, Tokai-works, of the Power Reactor and Nuclear Fuel Development Corporation (PNC) of Japan. The feed for the PNC runs was the highly active raffinate from reprocessing of spent fuel from fast breeder reactors. The PNC demonstration runs were planned without using the GTM. Results predicted by the GTM and those obtained experimentally by PNC for the three demonstration runs are compared. Effects of stage efficiency, nitrate complexation, temperature, and equipment type are also included.

I. INTRODUCTION

The Power Reactor and Nuclear Fuel Development Corporation (PNC) of Japan has been promoting actinides partitioning studies as part of efforts to develop advanced reprocessing systems. In the last two decades, PNC has recovered U and Pu from spent fuel by using the PUREX process. The PUREX process has allowed minor actinides (Am, Cm, and a fraction of the Np, Pu, and Cm) to remain in the high-level liquid waste (HLLW), which will be vitrified in their current program.

In recent studies [OZAWA-1992A, OZAWA-1993B, OZAWA-1992C], Ozawa et al. evaluated the option of separating all actinides from HLLW by using the TRUEX process. The main purpose of their studies was to verify the ability of the TRUEX process to treat actual highly active raffinate (HAR) that originated from reprocessing experiments using spent fuel from fast breeder reactors (FBR). At the Chemical Processing Facility, Tokai-works, five countercurrent flowsheet tests were conducted in which the TRUEX solvent was composed of 0.2M CMPO* and 1.0M tributyl phosphate (TBP) in n-dodecane. The feed was composed of HAR derived from PUREX reprocessing experiments of FBR-Joyo MK-II spent fuel burned up to ~54,000 MWD/T (megawatt-days per ton) and cooled for 2 to 4 years. The HAR was used without adjusting its acidity, but small amounts of plutonium and oxalic acid were added. Oxalic acid was added to inhibit Zr and Mo from coextraction with the actinides. The countercurrent experiments were conducted in mixer-settlers that had 19 stages for extraction/scrubbing and 16 to 19 stages for stripping and solvent regeneration. The volume holdup of one stage of the mixer-settler was 23 mL.

The purpose of this report is to compare the results predicted by the GTM [VANDEGRIFT] and the actual data published by PNC researchers for three of the countercurrent mixer-settler runs. The comparisons between the GTM predictions and the PNC measurements are useful in validating the GTM and showing where the model needs to be improved. They also show the value of the model in designing flowsheets, predicting extraction behavior, and showing effects of process upsets.

Table 1 shows the flowsheet conditions for three different countercurrent mixer-settler runs conducted by PNC prior to 1993 [OZAWA-1992A]. The hydrogen ion concentration for the feed was 4.0, 4.5, and 7.0M for Runs 1, 2, and 3, respectively. For Run 2, 0.02M $H_2C_2O_4$ was added to the feed, and ^{238}Pu was added as a tracer. The composition of the HAR is given in Table 2. The values reported by PNC for U, Np, Am, Cm, and Cs were estimated by using the ORIGEN-II code.

The concentration profiles were obtained for Runs 1, 2, and 3 and were compared to the predictions made by the GTM for given flowsheet conditions. For Run 1, only a concentration profile for HNO_3 was reported in the literature [OZAWA-1992B]. Profiles for Run 2 were obtained from the literature [OZAWA-1992B, OZAWA-1992C] and personal communication between Vandegrift and PNC [OZAWA-1993]. For Run 3, information was obtained from the literature [OZAWA-1992A].

---

* Octyl(phenyl)-N,N-diisobutylcarbamoylmethylphosphine oxide.

Table 1. Operating Conditions for PNC's Mixer-Settler Demonstration Runs

Run	Feed (HAR)	Solvent	Scrub - 1	Scrub - 2	Am strip	Np strip	Pu strip	U strip
1st	Joyo MK - II 54,100 MWD/T 1,500 d cooling H^+ = 4.0M 196 mL/h	0.2M CMPO 1.M TBP in n-dodecane 87 mL/h 8 stages	—	0.3M HNO_3 0.1M $H_2C_2O_4$ 40 mL/h 11 stages	—	—	0.01M HNO_3 106 mL/h 16 stages	—
2nd	Joyo MK-II 54,100 MWD/T 1,500 d cooling H^+ = 4.5M 0.02M $H_2C_2O_4$ ^{238}Pu addition 196 mL/h	0.2M CMPO 1.0M TBP in n-dodecane 119 mL/h 8 stages	7.7M HNO_3 0.03M $H_2C_2O_4$ 12 mL/h 6 stages	0.3M HNO_3 16 mL/h 5 stages	—	—	0.01M HNO_3 79 mL/h 16 stages	—
3rd	Joyo MK-II 54,100 MWD/T 1,500 d cooling + Joyo MK-II 54,700 MWD/T 700 d cooling H^+ = 7.0M 200 mL/h	0.2M CMPO 1.0M TBP in n-dodecane 100 mL/h 8 stages	7.7M HNO_3 0.03M $H_2C_2O_4$ 30 mL/h 6 stages	0.3M HNO_3 30 mL/h 5 stages	0.01M HNO_3 100 mL/h 5 stages	0.3M HNO_3 0.1M HAN 50 mL/h 5 stages	0.5M HNO_3 0.1M $H_2C_2O_4$ 50 mL/h 5 stages	0.1M Na_2CO_3 50 mL/h 4 stages

Table 2. Composition of the HAR[a]

Species	Concentration, M	Species	Concentration, M
U(VI)	7.1E-04[b]	Sm	4.5E-04
Np(V)	4.2E-05[c]	Eu	6.0E-05
Pu(IV)	6.7E-05[d]	Cs	2.3E-03
Am	5.0E-04[c]	Sr	5.1E-04
Cm	1.2E-06[c]	Zr	<3.3E-05[e]
Y	3.9E-04	Mo	1.2E-03
La	6.1E-04	Ru	3.1E-03
Ce	1.0E-03	Rh	2.5E-04
Pr	3.0E-04	Pd	<1.9E-05[e]
Nd	1.7E-03	Tc	2.1E-04

[a]Hydrogen ion concentration and additions are shown in Table 1 for each run.
[b]Estimated value corresponds to 0.5% loss in PUREX processing.
[c]Estimated value corresponds to no extraction in PUREX processing.
[d]Artificially added.
[e]Value lower than detection limit.

II. SUMMARY

The demonstration runs at PNC were performed without the TRUEX processing knowledge used in the United States and represented in the GTM. As a result, the PNC flowsheets had design problems, such as precipitation in the scrub section and not meeting processing goals in the stripping of plutonium.

Flowsheet conditions for the PNC countercurrent tests were simulated by using GTM versions 3.0.1 and 3.1. The primary difference between these two versions is that in version 3.1 we have added nitrate complexes of metal ions to our speciation calculations. The importance of that addition can be seen in Section IV. Our experience shows [BATTLES] that nitrate complexes cannot be ignored for high concentrations of rare-earth fission products in the feed. When nitrate complexes are neglected, the GTM predicts that far more free nitrate ion will be available than there actually is, causing the calculated distribution ratios to be much higher. As expected, the best fit was obtained for GTM version 3.1.

Four different stage efficiencies, 100%, 90%, 80%, and 70%, were simulated, and we concluded that the extraction/scrub section could best be simulated by 90% and the strip section by 100% efficiency. Fitting of the strip section data was less accurate. The GTM's predictions were compared to the results reported by PNC researchers [OZAWA-1992A, OZAWA-1992B, OZAWA-1992C, OZAWA-1993]. Species measured by PNC in the three runs were HNO_3, ^{242}Cm, ^{244}Cm, ^{241}Am plus ^{238}Pu, ^{239}Pu plus ^{240}Pu, ^{237}Np, ^{144}Ce, ^{155}Eu, ^{137}Cs, ^{125}Sb, ^{95}Zr, and ^{106}Ru. The concentration of ^{95}Zr was always under the detection limits. To validate the accuracy of the GTM for designing and simulating TRUEX processes, we compared the stagewise concentration profiles reported by PNC researchers to those predicted by the GTM (see Section III).

During our simulation, we encountered convergence problems in the modeling of the PNC demonstrations. These problems were traced to unrealistic zirconium concentrations being calculated for some of the stages. In our opinion, this problem occurred because PNC added inappropriate amounts of oxalic acid to the extraction and scrub sections. In general, oxalic acid is added to the feed to minimize the extraction of Zr, Mo, and Ru. Although the concentration of ^{95}Zr was under the detection limits in the PNC simulations, it is very likely that in the actual demonstrations, zirconium and perhaps other metal salts were "pinched" in the scrub and strip sections. Pinching means that the extraction factor is >1 in the first stage of a section and <1 in the last stage of the same section. Therefore, the concentration of these metals increased in both phases in all stages of the given section. Precipitation of oxalate was noted in the first PNC run [OZAWA-1992A]. In our effort to model the PNC runs, we lowered the concentration of zirconium in the feed, when necessary, to avoid convergence problems in the GTM. With 100% stage efficiency, the reduction in zirconium concentration was as high as eleven orders of magnitude for run 1, three orders of magnitude in run 2, and two orders of magnitude in run 3. Lowering the stage efficiency made these reductions less severe. At 90% stage efficiency, run 2 could be modeled with no reduction in zirconium feed concentration, but run 1 still required a reduction by nine orders of magnitude, and run 3 still required a reduction by two orders of magnitude.

In general, the results of our GTM simulation agree fairly well with the PNC experimental results for the extraction/scrub section. Predictions by the GTM for the rare earths were extremely accurate. For cesium, which is not extracted, the GTM's smallest distribution ratio (or D value) is set by convention at 1×10^{-3}. According to the PNC experimental data, this value should be 1×10^{-4}. For the case of ruthenium, comparison to the PNC experimental results indicates that the GTM is inaccurate if we assume that the ruthenium species are equilibrated. In calculating the distribution ratio of ruthenium in a stage, the GTM takes into account the type of contact equipment used by assuming that the contact time is a matter of a few seconds (a centrifugal contactor) or a minute or more (pulsed columns and mixer-settlers). The difference in modeling these types of contacting equipment is that we assume that (1) in a pulsed column or mixer-settler, the contact time between the organic and aqueous phases is long enough that ruthenium species have time to equilibrate, and (2) in the centrifugal contactor, no reequilibration can occur, and the speciation that is present in the feed remains constant throughout the flowsheet. To improve modeling of ruthenium behavior, we will need to collect extensive experimental data to model its distribution coefficient. This effort is not in our near-term plans.

For the strip section, simulated results generated by using version 3.1 of the GTM compare well with the experimental results reported by PNC researchers for curium and the rare earths. Calculational and experimental results for plutonium and neptunium showed less agreement than for the rare earths. The GTM assumes specific oxidation states for its calculations [Pu(III) or (IV) and Np(IV) or (V)]; the PNC data are reported as specific isotope concentrations only. Comparison of the experimental results and the GTM simulation for Pu(III) and Pu(IV) shows that experimental results are in better agreement with the Pu(IV) simulation. Neptunium stripping results in Run 3 are fitted much better by the GTM by assuming Np(IV) rather than Np(V). For the case of americium, predicted and experimental results were hard to compare. The americium experimental results were reported as ^{241}Am and ^{238}Pu since their alpha particle energies are very similar. In the case of the GTM, results are given for americium.

The effect of temperature was also calculated during the GTM simulation. Increasing the temperature has an adverse effect on the extraction section for Am, Cm, and the rare earths, because it decreases their distribution ratios, thus increasing their concentrations in the aqueous phase. For the strip section, an increase in temperature also decreases the distribution ratio, but, in this case, a lower distribution ratio increases the effectiveness of the strip section, lowering the organic phase concentration of those components that exit the strip section. The temperature effect on the plutonium distribution ratio was indirect. Although the effect of temperature on the distribution ratio for plutonium is too small to be included in the model that calculates the D value, a decrease in the distribution ratio for americium and the rare earths as the temperature increases will affect the concentration of plutonium in the aqueous phase. Because the process temperature was not controlled in the PNC runs, we looked at the effect that process temperature would have on the flowsheets. Results generated by the GTM show that 25°C gives the best fit for the extraction/scrub section and ≥55°C gives the best fit for the strip section.

III. GTM FLOWSHEET SETUP

Flowsheet conditions for PNC's countercurrent tests, given in Table 1, were simulated using the GTM [VANDEGRIFT] version 3.0.1. The HAR feed composition was as shown in Table 2. Since no information was available regarding stage efficiency for the mixer-settlers used by PNC, we simulated four different stage efficiencies, 100%, 90%, 80%, and 70%, to identify which stage efficiency best simulated the PNC experiments.

Convergence problems were encountered in modeling the PNC runs. These problems occurred, in our opinion, because PNC added inappropriate amounts of oxalic acid to the extraction and scrub sections in all runs. In general, oxalic acid is added to the feed to minimize the extraction of Zr and Ru. Although the concentration of ^{95}Zr was under the detection limits in the PNC runs, it is very likely that in the actual demonstrations, zirconium and perhaps other metal salts were pinched* in the scrub and strip sections. Precipitation of oxalate was noted in the first PNC run [OZAWA-1992A]. In our effort to model the PNC runs, we lowered the concentration of zirconium in the feed, when necessary, to avoid convergence problems in the GTM. Given in Table 3 are the values used for zirconium in the HAR feed to model each run using the GTM.

Table 3. Zirconium Concentration Used for the HAR Feed to Achieve Convergence in GTM Simulations

Run	Stage Efficiency, %	$[ZrO^{2+}]$, M[a]
1	100	3.30E-16
	90	3.30E-14
	80	3.30E-12
	70	3.30E-12
2	100	3.30E-08
	90	3.30E-05[b]
	80	3.30E-05[b]
	70	3.30E-05[b]
3	100	3.30E-07
	90	3.30E-07
	80	3.30E-07
	70	3.30E-07

[a]Zirconium composition for the HAR used in all PNC runs was 3.3E-05M.

[b]Same value as in PNC Run 2.

* Pinching means that the extraction factor was >1 in the first stage of a section and <1 in the last stage of the same section. Therefore, the concentration of these metals increased in both phases in all stages of the given section.

The GTM did not converge in these cases because a large zirconium buildup in the scrub section caused the calculation to predict unrealistic aqueous phase compositions in that section for all stage efficiencies and in the strip section for Run 2 at 100% stage efficiency. To understand these pinching problems, it is necessary to look at the zirconium, hydrogen ion,* and oxalate concentration profiles. In Fig. 1, we show the concentration profile for zirconium in Runs 1 and 2 at 90% stage efficiency. Notice how zirconium is being pinched in the scrub (stages 9-19) in Run 1 and in the strip (stages 20-35) in Run 2. When no fluoride is present in the feed, the distribution ratio for zirconium can be written in terms of the activity of nitrate (which is a function of HNO_3 concentration), and the concentration of free zirconium (which is a function of oxalate concentration). The concentration profile for hydrogen ion for Run 1 and 2 at 90% stage efficiency is given in Fig. 2. Also shown in this figure is the experimental aqueous phase concentration profile obtained by PNC. The concentration profile for oxalate ion for Run 1 and 2 at 90% stage efficiency is given in Fig. 3.

In Run 1, the concentration of both hydrogen ion and oxalate in both phases remains constant in the extraction section (left side in Figs. 2 and 3). The distribution coefficient for zirconium (D_{Zr}) in this section increases from 57 to 73 between stage 1 and stage 8. The organic to aqueous flow ratio (O/A) for this section is 0.37. So, for the extraction section, the extraction factor for zirconium, defined as the product of the O/A ratio and D_{Zr}, is much greater than one — causing zirconium to report to the organic phase (left, Fig. 1). For the scrub section, the acid aqueous phase concentration decreases, causing the distribution coefficient for zirconium to decrease from 37 in the first scrub stage to 0.001 in the last stages. The extraction factor goes from being much greater than one in the first stages of the scrub to being much less than one in the last stages of the scrub, causing zirconium to build up in both phases.

In Run 2, the buildup in zirconium is not seen in the scrub, but in the strip section (right, Fig. 1). For this case, enough oxalate was present in the feed (right, Fig. 3) to prevent the extraction of zirconium (indicated by the constant concentration profile in stages 1 to 8 in the left half of Fig. 1). Much of the oxalate was scrubbed from the organic phase in the latter scrub stages. As the oxalate concentration continues to decrease in the strip section (right, Fig. 3, stages 20-35), the concentration of uncomplexed zirconium increases, causing the distribution coefficient to increase and the extraction factor to become greater than one as a result of the high concentration of nitrate in the aqueous phase. Because the nitric acid concentration is decreasing in the strip section (right, Fig. 2, stages 20-35), the decreasing effect of nitrate on the zirconium distribution coefficient quickly overcomes the maximum effect of free or uncomplexed zirconium equaling the total zirconium present in the aqueous phase. As the distribution coefficient for zirconium begins to decrease, the extraction factor becomes less than one. Therefore, the extraction factor goes from being much greater than one, in the first stage of the strip section, to being much less than one, in the last stages of the strip section, causing zirconium to build up in both phases.

---

* In the GTM, this includes free $[H^+]$ and hydrogen associated with all acidic species (i.e., $H_2C_2O_4$, $HC_2O_4^-$, HF, etc.).

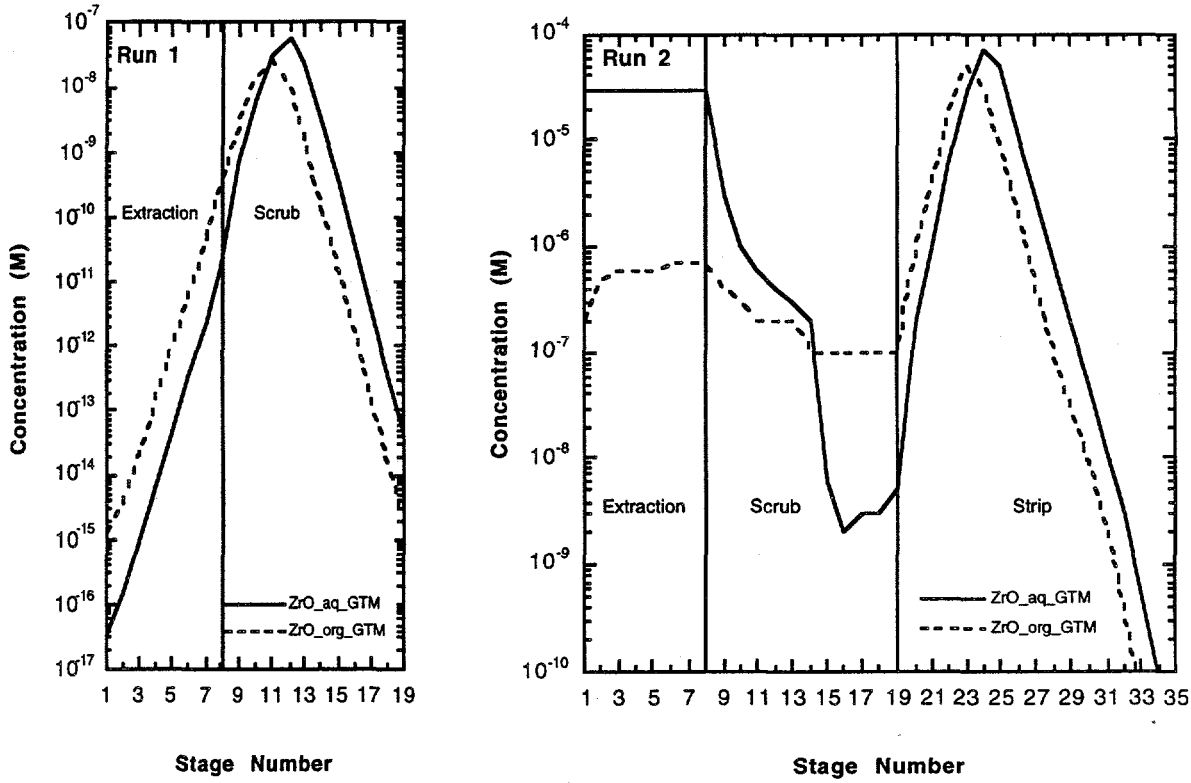

Fig. 1. Stagewise Aqueous and Organic Phase Concentration Profile for Zirconium in the Extraction/Scrub and Strip Sections. Shown in these figures are the GTM simulations for 90% stage efficiency for PNC Run 1 (left) and Run 2 (right).

The version of the GTM used in the initial simulation, version 3.0.1, did not account for nitrate complexation. As a result, the GTM overestimated the amount of rare earths being stripped. In the new version of the GTM, version 3.1, we have added nitrate complexation, and we no longer overestimate stripping for the rare earths. The two versions are compared in the next section.

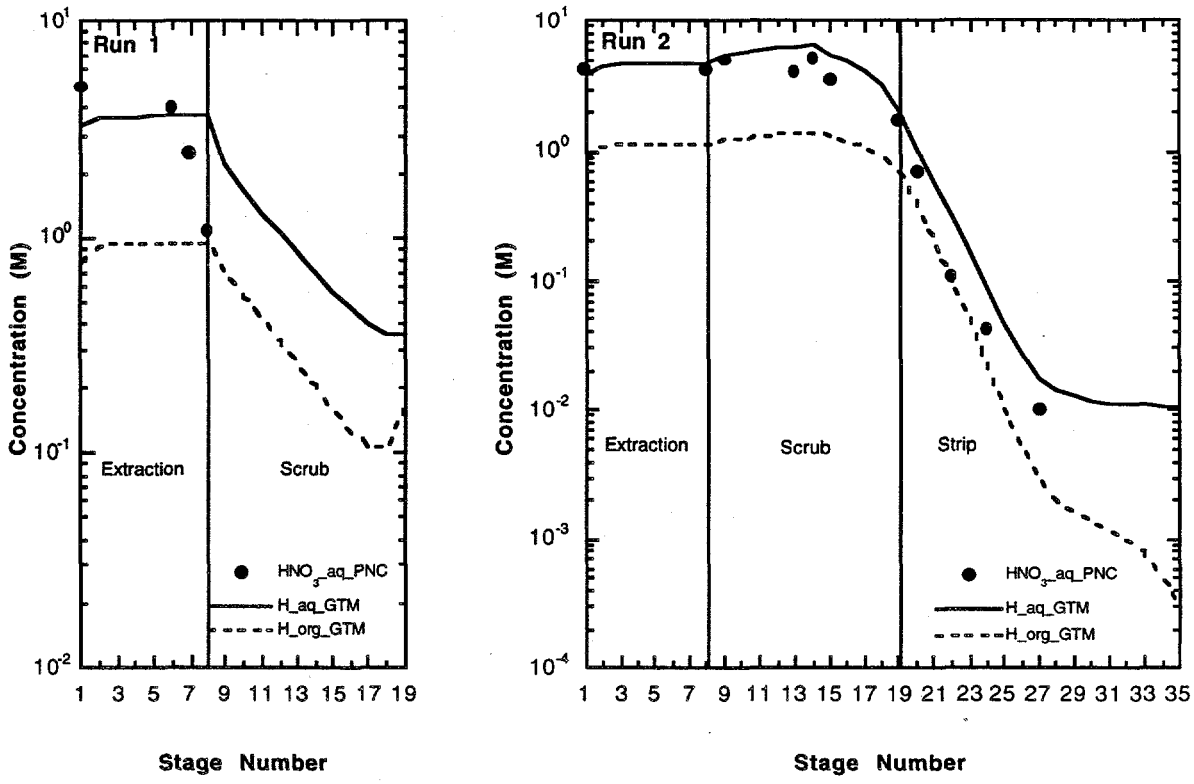

Fig. 2. Stagewise Aqueous and Organic Phase Concentration Profile for Hydrogen Ion in the Extraction/Scrub and Strip Sections. Shown in these figures are the GTM simulations for 90% stage efficiency for PNC Run 1 (left) and Run 2 (right), and the experimental aqueous phase nitric acid concentration results obtained for these runs.

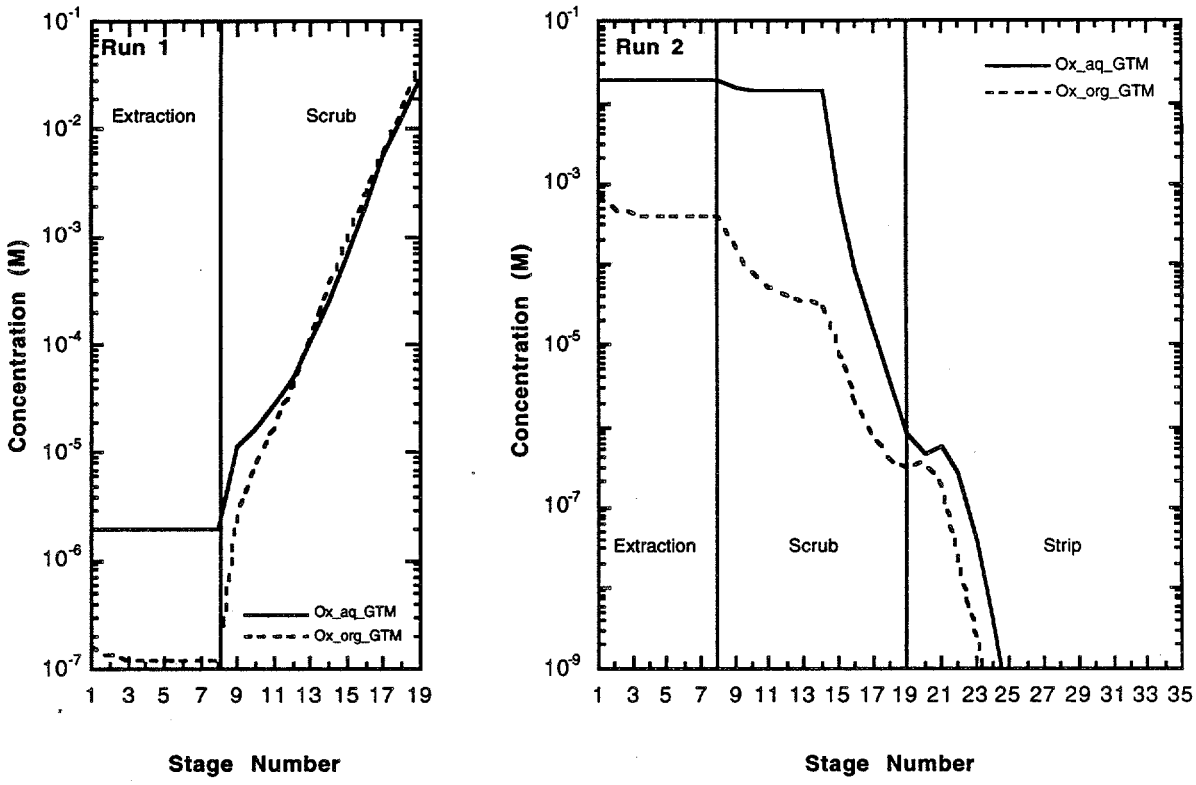

Fig. 3. Stagewise Aqueous and Organic Phase Concentration Profile for Oxalate Ion in the Extraction/Scrub and Strip Sections. Shown in these figures are the GTM simulations for 90% stage efficiency for Run 1 (left) and Run 2 (right).

IV. RESULTS AND COMPARISONS

The simulation results were compared to all the results reported by PNC researchers prior to 1993 [OZAWA-1992A, OZAWA-1992B, OZAWA-1992C, OZAWA-1993]. Stagewise data were collected on the behavior of nitric acid and several fission-product and actinide radioisotopes during their runs; Run 2 was the best documented and the one with which most comparisons were made. Species measured by PNC in the three runs were HNO_3, ^{242}Cm, ^{244}Cm, ^{241}Am plus ^{239}Pu, ^{239}Pu plus ^{240}Pu, ^{237}Np, ^{144}Ce, ^{155}Eu, ^{137}Cs, ^{125}Sb, ^{95}Zr, and ^{106}Ru. The concentration of ^{95}Zr was always under the detection limits. In general, the GTM predictions correlated well with experimental results for the runs, especially for the rare-earth fission products, americium, and curium. Differences between model predictions and experimental data were analyzed in terms of the process chemistry and demonstration conditions.

The PNC experimental results were reported in becquerels per milliliter (Bq/mL), while the GTM results are obtained in moles per liter (M). To compare the two profiles, we converted the GTM results to the equivalent values in becquerels per milliliter. Many of the PNC results were reported as either specific isotope concentrations or as a combination of two isotopes, and since the ratio of these isotopes was not reported, it was not possible to convert the concentration profiles by using specific activities. The GTM always assumes specific oxidation states for its calculations, so to compare the results for the extraction/scrub section, (1) we took an average of the ratio of the concentration reported by PNC in the organic phase of either the extraction or scrub section (depending on the component, whichever was almost a constant) and that predicted by the GTM and then (2) multiplied the concentration profile predicted by the GTM for both phases in the extraction/scrub section by the ratio calculated in (1). We then compared the simulated profiles to the PNC results. To compare the strip section, (1) we took the ratio of the organic concentration reported by PNC in the first stage and that predicted by the GTM for that stage and section and then (2) multiplied the concentration profile predicted by the GTM for both phases in the whole strip section by the ratio calculated in (1). We then compared the simulated profiles with the PNC results. When PNC reported no values in the first organic stage for the strip, the next available stage was used.

A. Run 1

The only results reported in the literature for Run 1 are for nitric acid concentration in the aqueous phase [OZAWA-1992B]. In Fig. 4, we have plotted the molar concentration of hydrogen ion in the aqueous phase predicted by the GTM versus the stage number for 90% stage efficiency. Also shown in this plot is the experimental concentration profile given by PNC [OZAWA-1992B], identified as [HNO_3]. The GTM predictions shown in Fig. 4 were calculated by using version 3.1 of the GTM, which includes nitrate complexation.

Figure 4 indicates some discrepancies between the GTM and PNC results. Because we are unfamiliar with the way in which this nitric acid profile was obtained experimentally, it is difficult to establish a reason for this discrepancy. We can only speculate that there could have been an error when the aqueous phase solution was titrated. Many metals in solution hydrolyze, and their effect needs to be accounted for when calculating the experimental results.

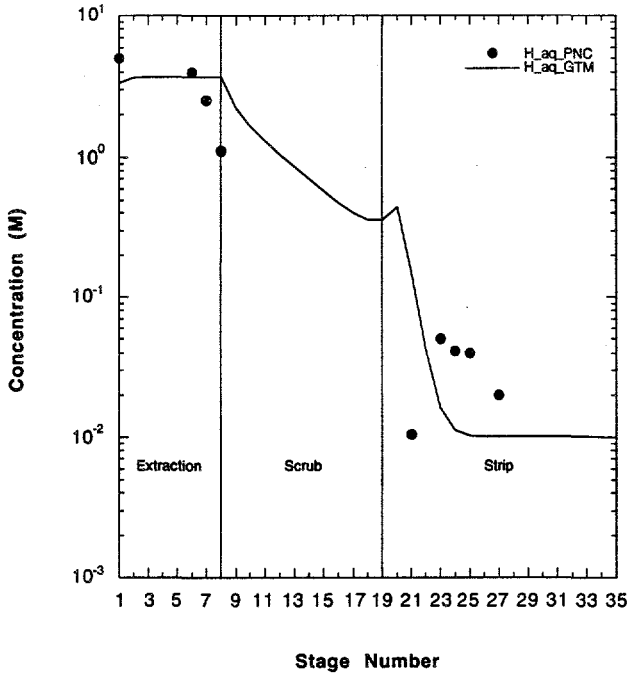

Fig. 4. Stagewise Aqueous Phase Concentration Profile for Hydrogen Ion in the Extraction/Scrub and Strip Sections. Shown in this figure are the GTM simulation for 90% stage efficiency for Run 1 and the experimental results obtained for this run.

B. Run 2

1. Extraction/Scrub and Strip Results

We analyzed in detail the results reported for Run 2 [OZAWA-1992B, OZAWA-1992C, OZAWA-1993], since most of the PNC results published are for this run. Version 3.0.1 of the GTM was used to simulate the results given in this section (VI.B.1). The extraction/scrub profiles for Ce, Eu, Cs, and Ru obtained by the GTM for Run 2 are given in Figs. 5-8. In these figures, we have plotted the concentration predicted by the GTM versus the stage number for both aqueous and organic phases in the extraction/scrub sections. Also given in these plots are the experimental concentration profiles reported by PNC. All figures correspond to a stage efficiency of 90%; after simulating four different stage efficiencies, 100%, 90%, 80%, and 70%, we concluded that 90% would most accurately simulate the extraction/scrub section of the experiments. In Fig. 9, we compare the concentration profiles obtained for cerium using the GTM at four different stage efficiencies versus the PNC experimental results. A stage efficiency of 90% best describes the experimental results for both aqueous and organic phases. Similar results were obtained for Eu and Cs in the extraction/scrub section. For ruthenium, the GTM predicted that it would be extracted, but the PNC experimental results indicated the contrary (Fig. 8); therefore, ruthenium was not used to establish a stage efficiency for the extraction/scrub section.

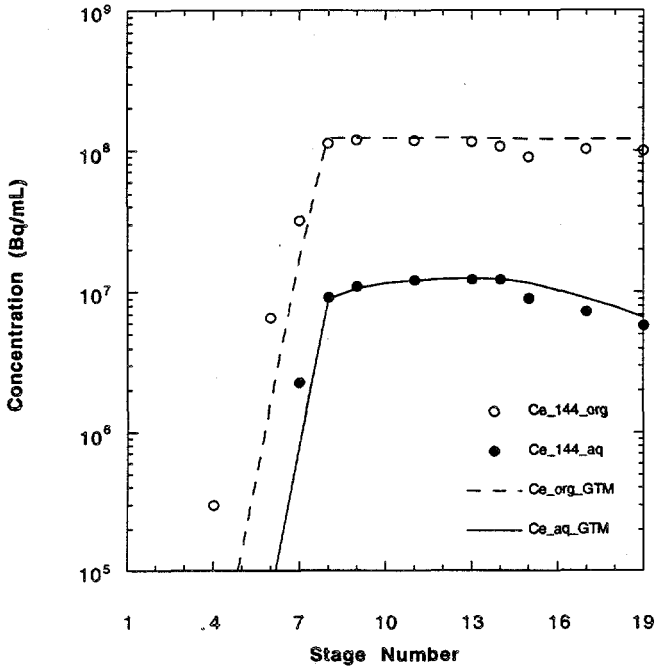

Fig. 5. Stagewise Aqueous and Organic Phase Concentration Profile for Cerium in the Extraction/Scrub Section. Shown in this figure are the GTM simulation for 90% stage efficiency for Run 2 and the experimental results obtained for this run.

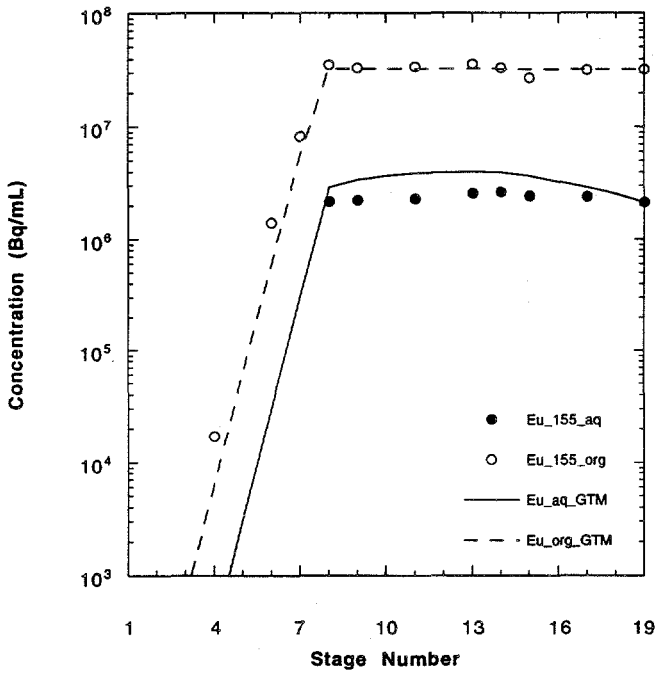

Fig. 6. Stagewise Aqueous and Organic Phase Concentration Profile for Europium in the Extraction/ Scrub Section. Shown in this figure are the GTM simulation for 90% stage efficiency for Run 2 and the experimental results obtained for this run.

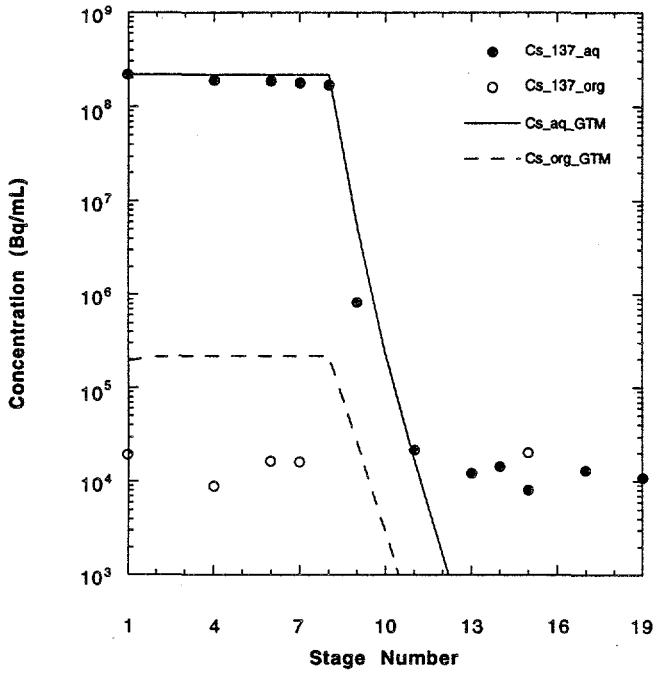

Fig. 7. Stagewise Aqueous and Organic Phase Concentration Profile for Cesium in the Extraction/Scrub Section. Shown in this figure are the GTM simulation for 90% stage efficiency for Run 2 and the experimental results obtained for this run.

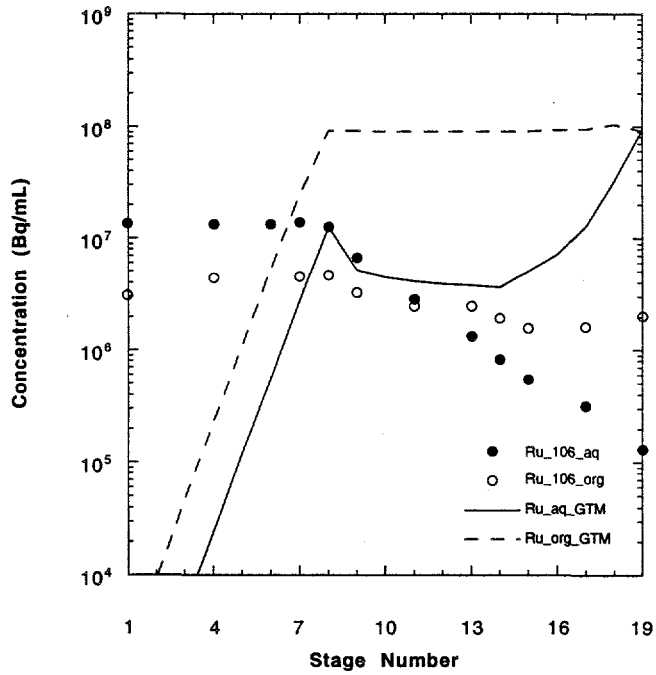

Fig. 8. Stagewise Aqueous and Organic Phase Concentration Profile for Ruthenium in the Extraction/ Scrub Section. Shown in this figure are the GTM simulation for 90% stage efficiency for Run 2 and the experimental results obtained for this run.

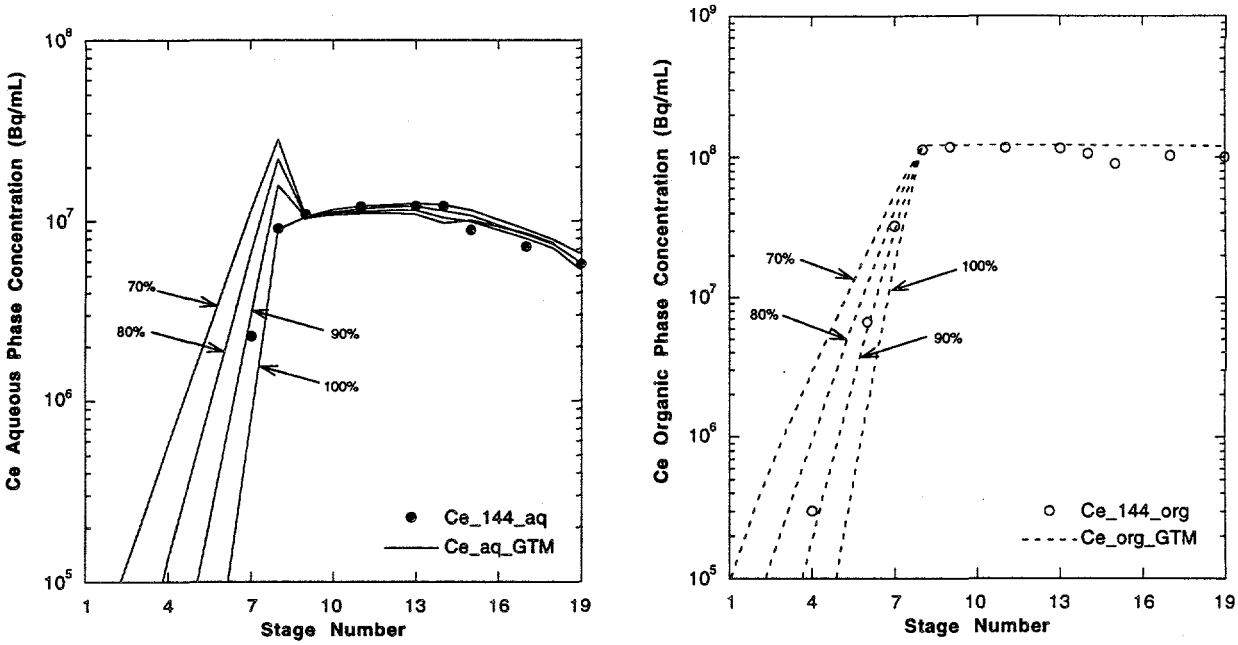

Fig. 9. Stagewise Aqueous and Organic Phase Concentration Profile for Cerium as a Function of Stage Efficiency for the Extraction/Scrub Section. Shown in these figures are the GTM simulations for 70%, 80%, 90%, and 100% stage efficiency for Run 2 for the aqueous (left) and organic (right) phase and the experimental results obtained for this run.

For the extraction/scrub section, the results of our GTM calculations fit the experimental data fairly well, in general (Figs. 5, 6, and 7). For Ce and Eu, the GTM predicts the same behavior for both components (Figs. 5 and 6) because it uses the same model to calculate distribution coefficients for all the rare earths. Prediction by the GTM for the rare earths is extremely accurate (Figs. 5 and 6). For cesium (Fig. 7), which is not extracted, the GTM's smallest D value is set by convention at 1×10^{-3}. According to the PNC experimental data, this value should be 1×10^{-4}. For ruthenium, as discussed above, the GTM predicted that it would be extracted, but comparison to the PNC results (Fig. 8) indicates that the GTM's model is inaccurate, if we assume that the ruthenium species are equilibrated. The distribution coefficient for ruthenium is a function of the contact time; therefore, it is dependent on the type of equipment used. The effect of the different contact times (or equipment type) is covered in detail in Section IV.B.4.

For the strip section, the profiles obtained by the GTM for Run 2 are given in Figs. 10-15. In these figures, we have plotted the concentration predicted by the GTM versus the stage number for both aqueous and organic phases. Also given in Figs. 12 through 15 are the experimental concentration profiles reported by PNC. Note that in Figs. 10 and 11, Am and Pu experimental results are reported as a combination of ^{241}Am plus ^{238}Pu (Fig. 10) and ^{239}Pu plus ^{240}Pu (Fig. 11). Since the ratio of these isotopes was not reported, it was not possible to simulate the different isotopes. For the GTM simulation, it

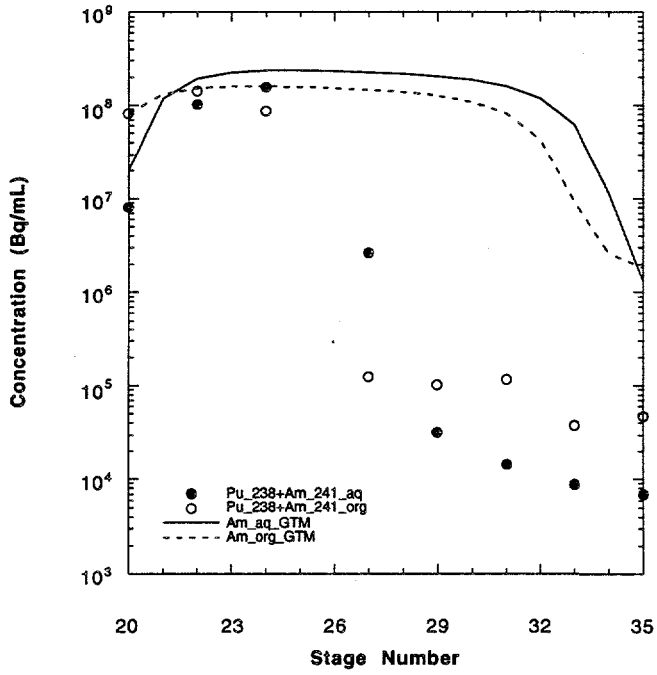

Fig. 10. Stagewise Aqueous and Organic Phase Concentration Profile for Americium in the Strip Section. Shown in this figure are the GTM simulation for americium(III) at 100% stage efficiency for Run 2 and the experimental results obtained for ^{241}Am plus ^{238}Pu for this run.

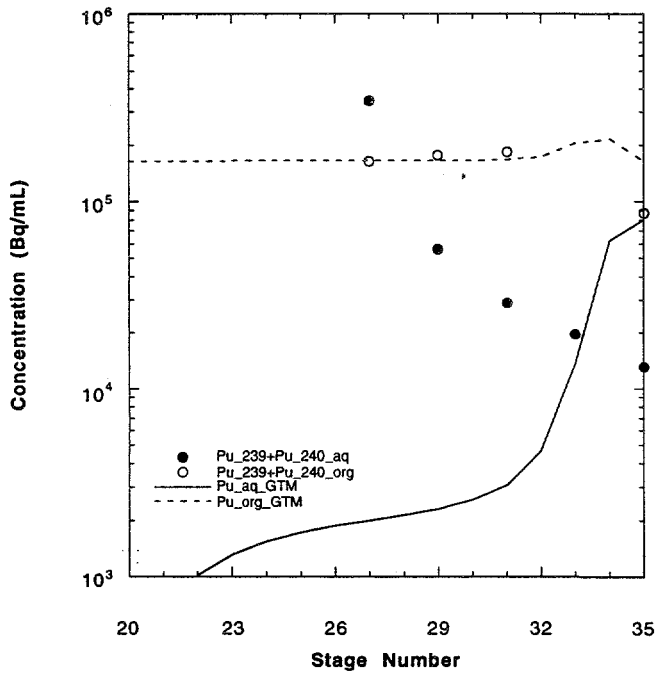

Fig. 11. Stagewise Aqueous and Organic Phase Concentration Profile for Plutonium in the Strip Section. Shown in this figure are the GTM simulation for plutonium(IV) at 100% stage efficiency for Run 2 and the experimental results obtained for ^{239}Pu plus ^{240}Pu for this run.

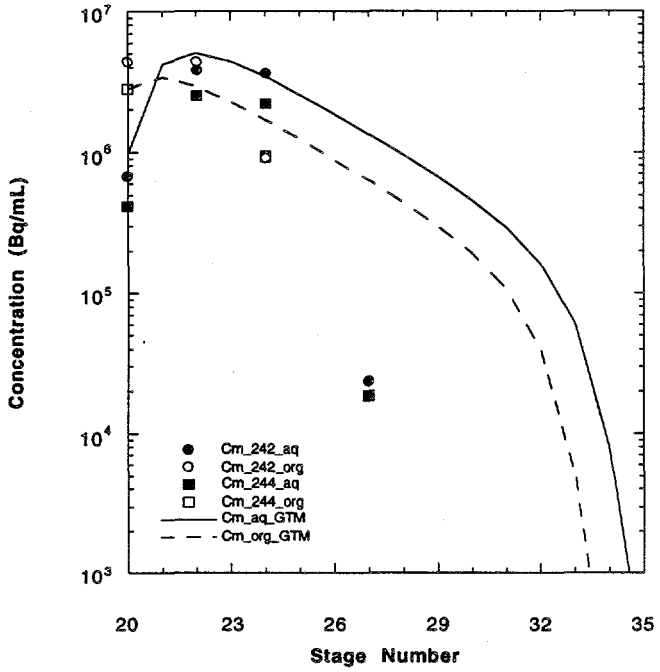

Fig. 12. Stagewise Aqueous and Organic Phase Concentration Profile for Curium in the Strip Section. Shown in this figure are the GTM simulation for 100% stage efficiency for Run 2 and the experimental results obtained for this run.

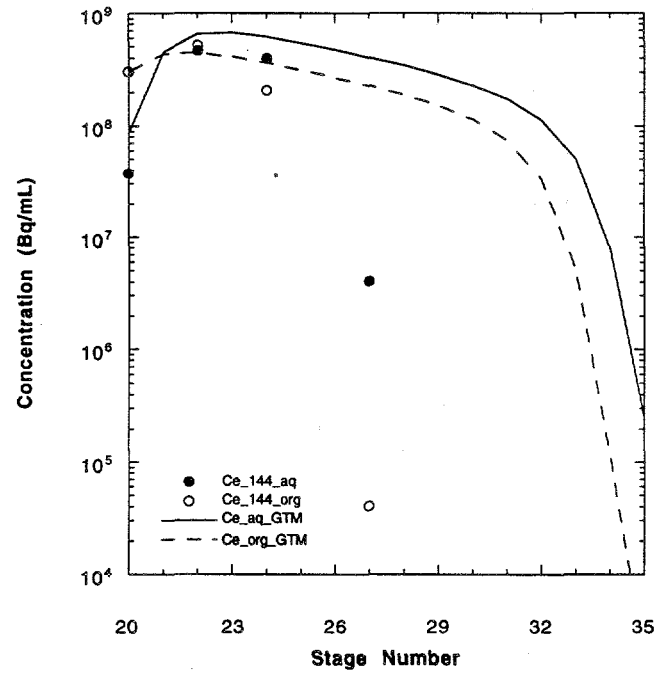

Fig. 13. Stagewise Aqueous and Organic Phase Concentration Profile for Cerium in the Strip Section. Shown in this figure are the GTM simulation for 100% stage efficiency for Run 2 and the experimental results obtained for this run.

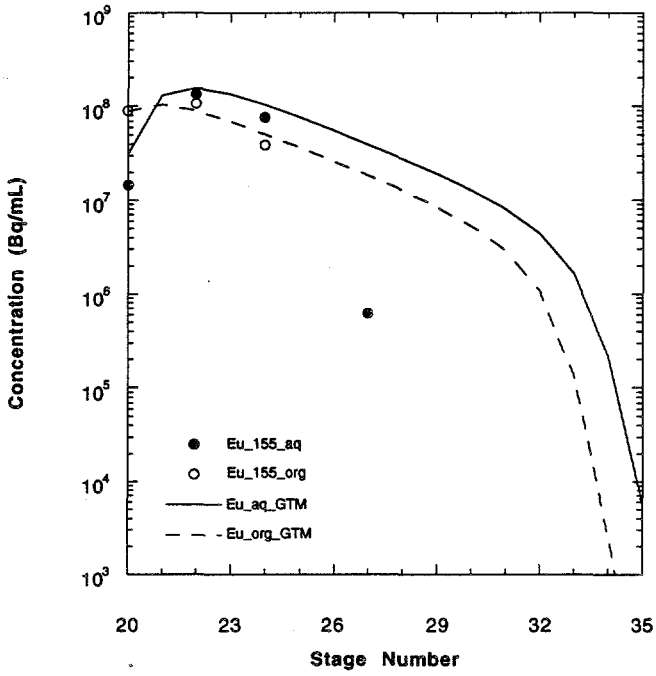

Fig. 14. Stagewise Aqueous and Organic Phase Concentration Profile for Europium in the Strip Section. Shown in this figure are the GTM simulation for 100% stage efficiency for Run 2 and the experimental results obtained for this run.

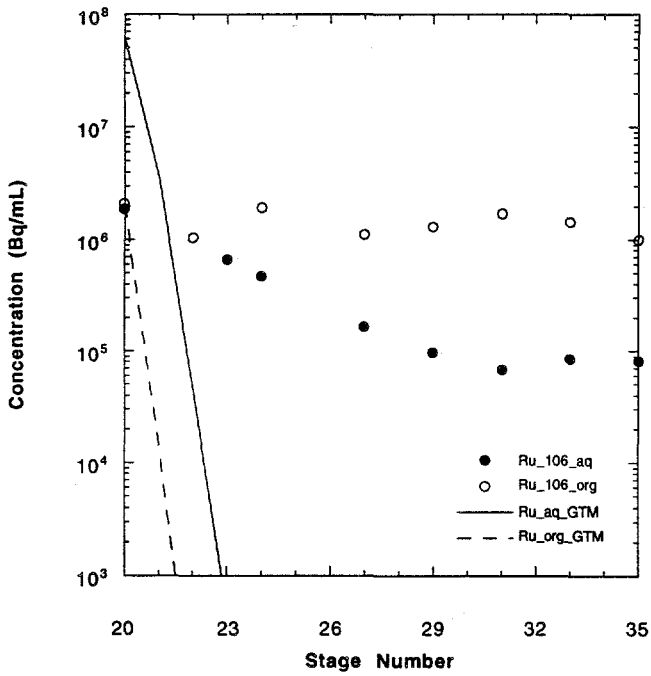

Fig. 15. Stagewise Aqueous and Organic Phase Concentration Profile for Ruthenium in the Strip Section. Shown in this figure are the GTM simulation for 100% stage efficiency for Run 2 and the experimental results obtained for this run.

was assumed that all the americium was Am^{3+} and all the plutonium was Pu^{4+}. Concentration profiles obtained by the GTM under that assumption are given in Figs. 10 and 11. All figures reported for the strip section correspond to a stage efficiency of 100%. After simulating four different stage efficiencies, 100%, 90%, 80%, and 70%, we concluded that 100% best simulated the strip section of the PNC experiments. In Fig. 16, we compare the concentration profiles obtained for cerium using the GTM at four different stage efficiencies with the PNC experimental results. Notice in Fig. 16 how a stage efficiency of 100% best describes the experimental results for both aqueous and organic phases. Although similar results were obtained for Am, Cm, Ce, and Eu, fitting of the strip section data was less accurate. As for the extraction section, ruthenium was not used to establish stage efficiency.

For the strip section, the comparison indicates that the GTM underestimates americium stripping in the presence of high concentrations of rare earths (Fig. 10). This problem was also found in modeling the Mark 42 targets from Oak Ridge National Laboratory (ORNL) [BATTLES]. The comparison between the GTM and the PNC experimental results for plutonium are given in Fig. 11. The discrepancy in the results occurred because we assume that all the plutonium exiting the scrub section was Pu(IV). By assuming that all the plutonium entering the strip section has been reduced to Pu(III), we would obtain a concentration profile for the strip, for both the organic and the aqueous phase, very much like those obtained for Am(III) (Fig. 10). Results similar to those for Am were obtained for Cm, Ce, and Eu (Figs. 12-14). The underestimation of Am, Cm, and

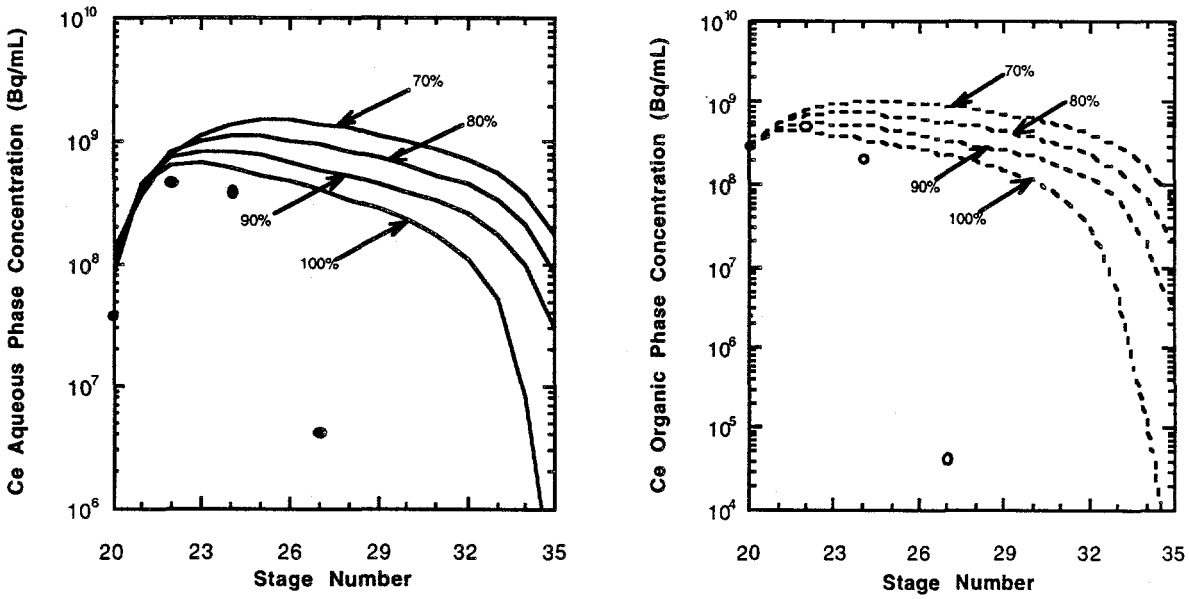

Fig. 16. Stagewise Aqueous and Organic Phase Concentration Profile for Cerium as a Function of Stage Efficiency for the Strip Section. Shown in these figures are the GTM simulations for 70%, 80%, 90%, and 100% stage efficiency for Run 2 for the aqueous (left) and organic (right) phase and the experimental results obtained for this run.

rare-earth stripping occurred because the nitrate activity in the aqueous strip solutions was overestimated. We were ignoring the rare earth-nitrate complexes, which act to lower the available uncomplexed, or free, nitrate. Nitrate complexation was added to the GTM in version 3.1. Results reflecting the inclusion of nitrate complexation are given in the next section.

The differences between GTM predictions and the PNC results for stripping of rare earths, Am, and Cm could also be explained if the flow rate in the aqueous strip solution was higher than reported in Table 1. As we did for stage efficiency, different aqueous strip flow rates could be simulated to find which best described the PNC experimental results for this section.

2. Nitrate Complexation

All the flowsheets results given in Section IV.B.1 (Figs. 5-16) were simulated by using GTM version 3.0.1, which did not account for nitrate complexation. By including nitrate complexes in version 3.1, we have significantly improved the GTM's fit to the PNC stripping data for Am, Cm, Ce, and Eu, as shown in Figs. 17-20.

We have also included in Fig. 21, for comparison purposes, the curium concentration profile calculated by both versions of the GTM for the TRUEX flowsheet used for processing the Mark 42 targets from ORNL [BATTLES]. The basic TRUEX flowsheet for processing the Mark 42 targets is given in Fig. 22. The experimental values

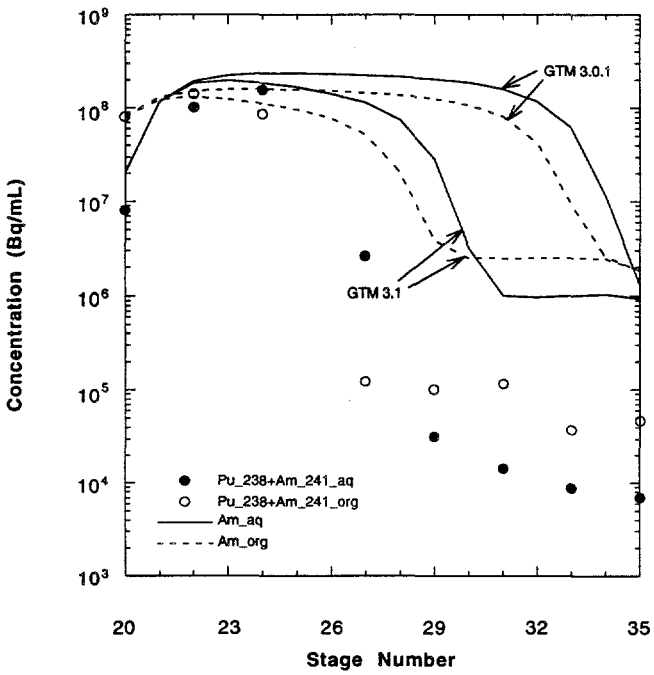

Fig. 17. Stagewise Aqueous and Organic Phase Concentration Profile for Americium in the Strip Section. Shown are the GTM simulation for americium(III) at 100% stage efficiency for Run 2 calculated using GTM versions 3.0.1 and 3.1 and the experimental results obtained for ^{241}Am plus ^{238}Pu for this run.

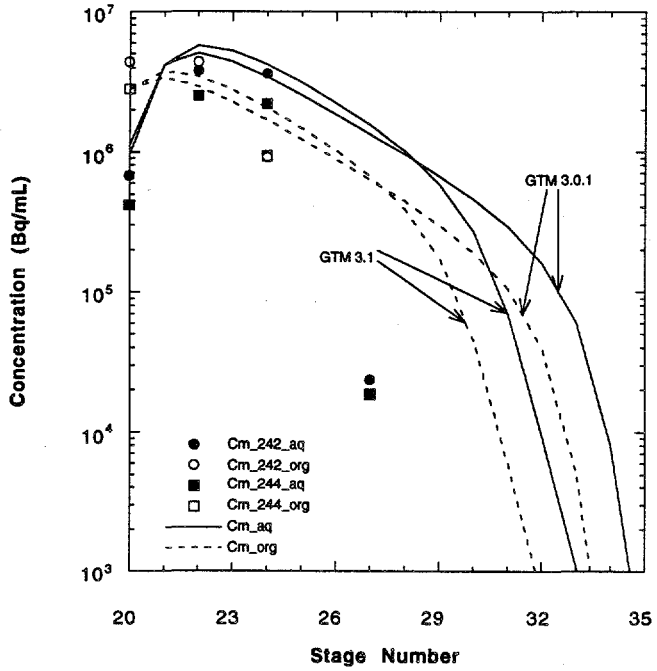

Fig. 18. Stagewise Aqueous and Organic Phase Concentration Profile for Curium in the Strip Section. Shown are the GTM simulation for 100% stage efficiency for Run 2 calculated using GTM versions 3.0.1 and 3.1 and the experimental results obtained for this run.

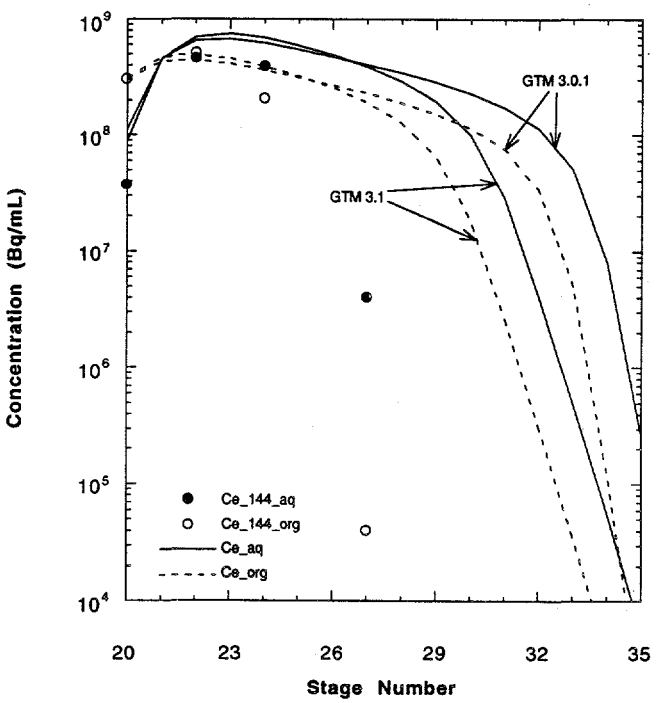

Fig. 19. Stagewise Aqueous and Organic Phase Concentration Profile for Cerium in the Strip Section. Shown are the GTM simulation for 100% stage efficiency for Run 2 calculated using GTM versions 3.0.1 and 3.1 and the experimental results obtained for this run.

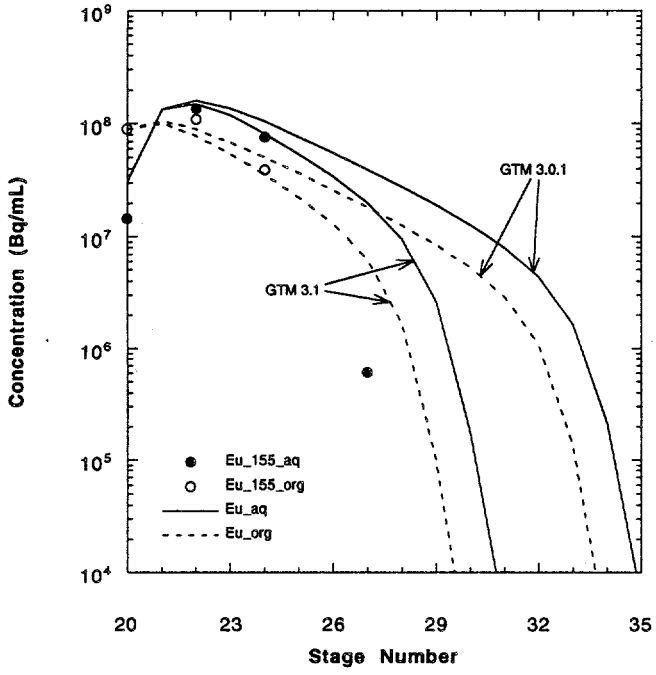

Fig. 20. Stagewise Aqueous and Organic Phase Concentration Profile for Europium in the Strip Section. Shown are the GTM simulation for 100% stage efficiency for Run 2 calculated using GTM versions 3.0.1 and 3.1 and the experimental results obtained for this run.

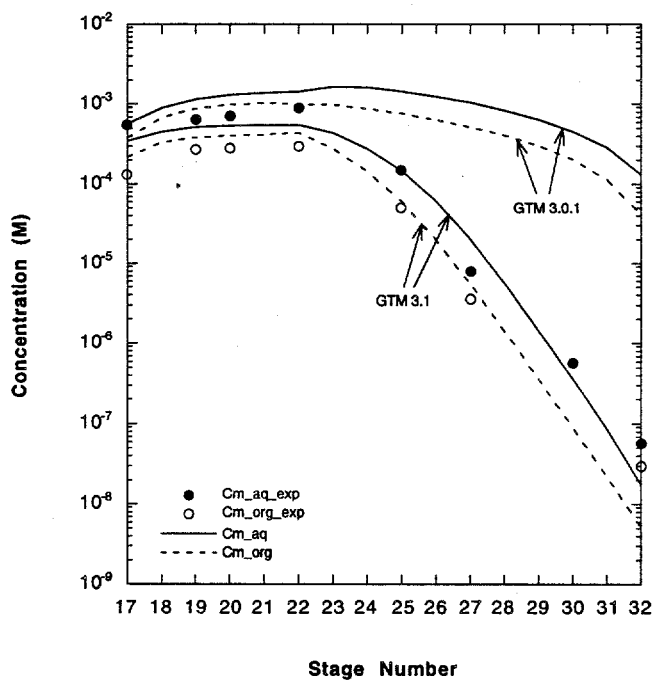

Fig. 21. Stagewise Aqueous and Organic Phase Concentration Profile for Curium in the Strip Section for Mark 42 Targets. Shown are the GTM simulation for the basic TRUEX flowsheet for processing Mark 42 targets from ORNL (given in Fig. 22) calculated using GTM versions 3.0.1 and 3.1 and the experimental results obtained by ORNL.

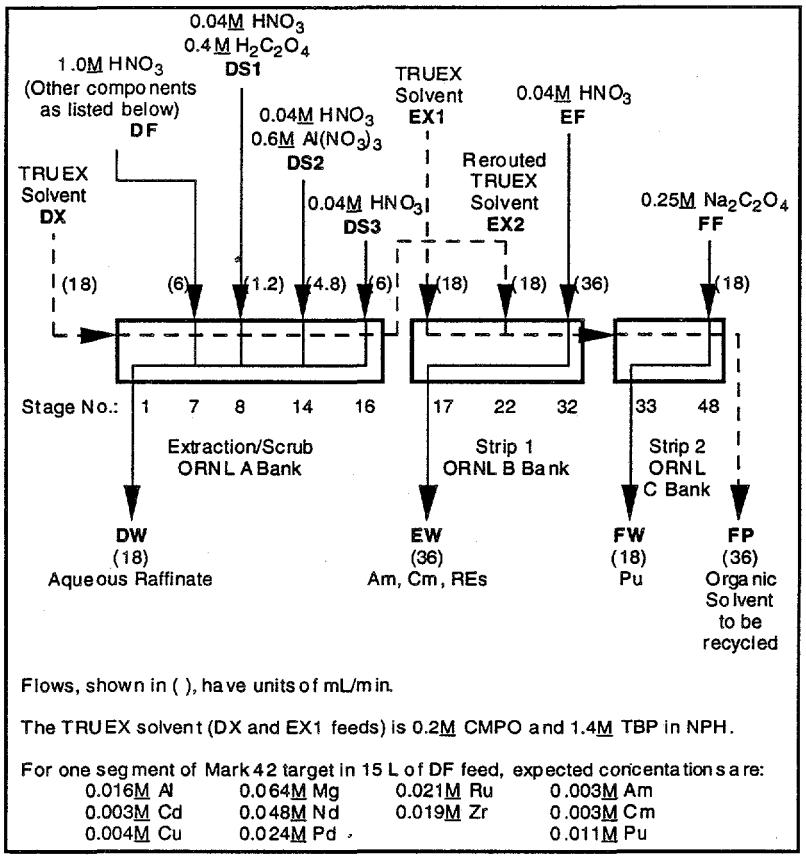

Fig. 22. Basic TRUEX Flowsheet for Processing Mark 42 Targets from ORNL. The symbol "REs" represents "rare earths."

obtained for the first strip section by ORNL when processing their basic TRUEX flowsheet [FELKER] are shown in Fig. 21. Note the improved accuracy of the results predicted by version 3.1, which includes nitrate complexation.

3. Temperature

Temperature effects on the concentration profile for Run 2 at 90% stage efficiency can be seen in Figs. 23 and 24 for the extraction section for Ce and Eu, and in Figs. 25-29 for the strip section for Am, Pu, Cm, Ce, and Eu. All temperature effects were modeled using version 3.1 of the GTM. Since our fit of the extraction/scrub section was more accurate than our fit of the strip section, for consistency all flowsheet calculations were done using 90% stage efficiency for all sections (instead of using 90% for the extraction/scrub and 100% for the strip). Increasing the temperature decreases the distribution coefficient calculated by the GTM for Am, Cm, and the rare earths (Ce and Eu). A stagewise profile of the distribution coefficient for americium as a function of

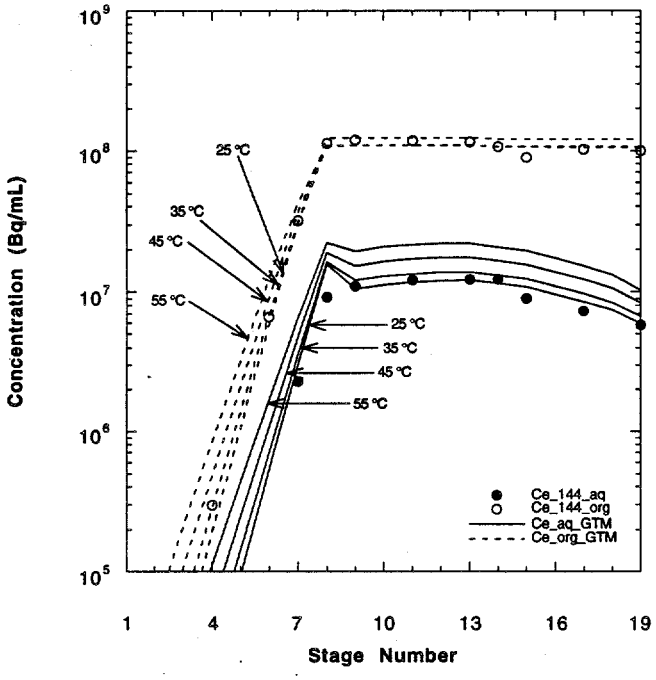

Fig. 23. Stagewise Aqueous and Organic Phase Concentration Profile for Cerium as a Function of Temperature for the Extraction/Scrub Section. Shown in this figure are the GTM simulations for 25°C, 35°C, 45°C, and 55°C at 90% stage efficiency for Run 2 and the experimental results obtained for this run.

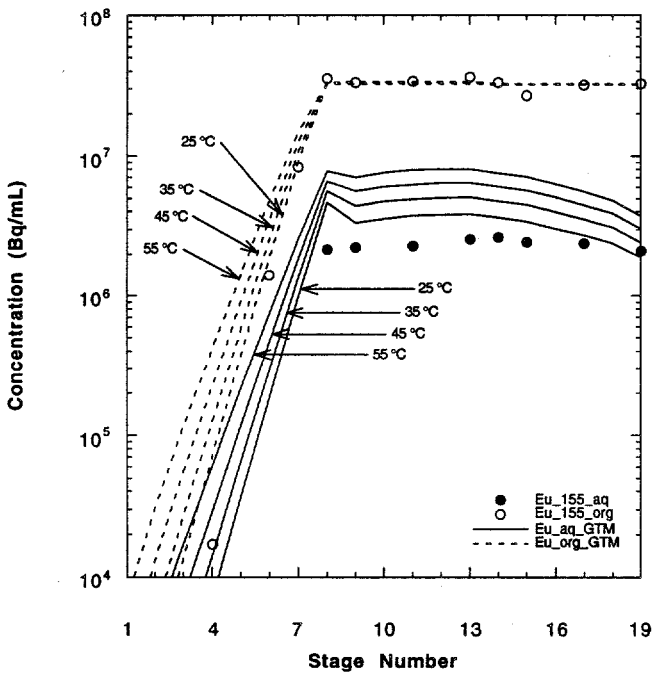

Fig. 24. Stagewise Aqueous and Organic Phase Concentration Profile for Europium as a Function of Temperature for the Extraction/Scrub Section. Shown in this figure are the GTM simulations for 25°C, 35°C, 45°C, and 55°C at 90% stage efficiency for Run 2 and the experimental results obtained for this run.

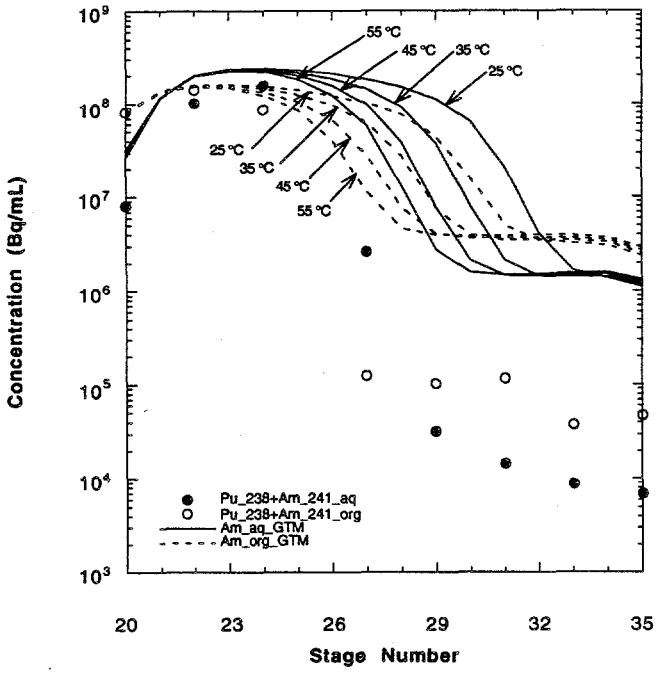

Fig. 25. Stagewise Aqueous and Organic Phase Concentration Profile for Americium as a Function of Temperature for the Strip Section. Shown in this figure are the GTM simulations for 25°C, 35°C, 45°C, and 55°C for americium(III) at 90% stage efficiency for Run 2 and the experimental results obtained for ^{241}Am plus ^{238}Pu for this run.

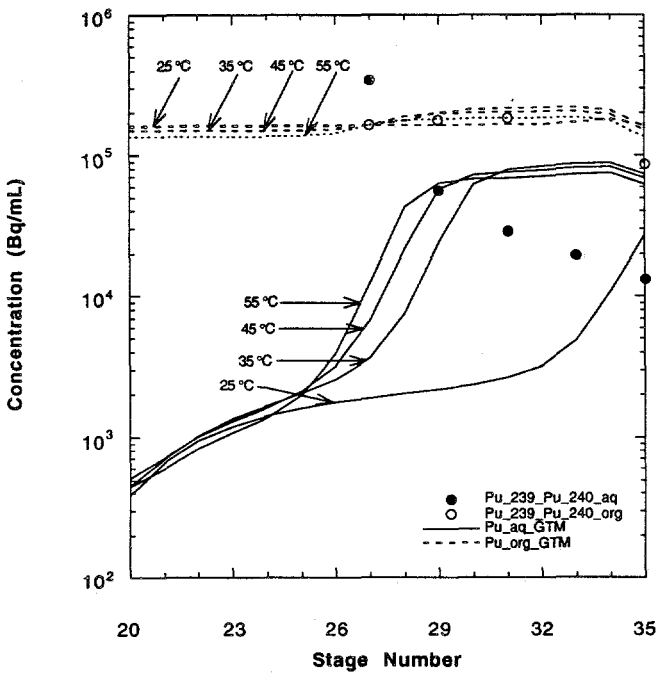

Fig. 26. Stagewise Aqueous and Organic Phase Concentration Profile for Plutonium as a Function of Temperature for the Strip Section. Shown in this figure are the GTM simulations for 25°C, 35°C, 45°C, and 55°C for plutonium(IV) at 90% stage efficiency for Run 2 and the experimental results obtained for ^{239}Pu plus ^{240}Pu for this run.

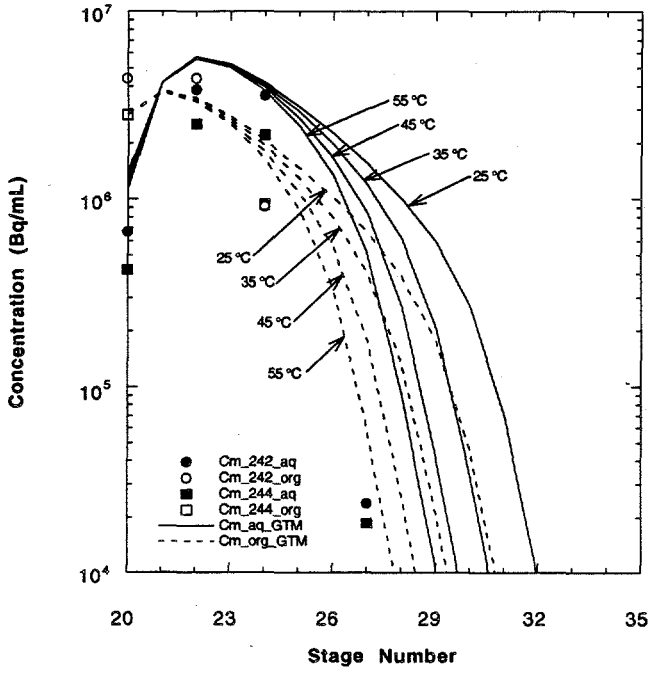

Fig. 27. Stagewise Aqueous and Organic Phase Concentration Profile for Curium as a Function of Temperature for the Strip Section. Shown in this figure are the GTM simulations for 25°C, 35°C, 45°C, and 55°C at 90% stage efficiency for Run 2 and the experimental results obtained for this run.

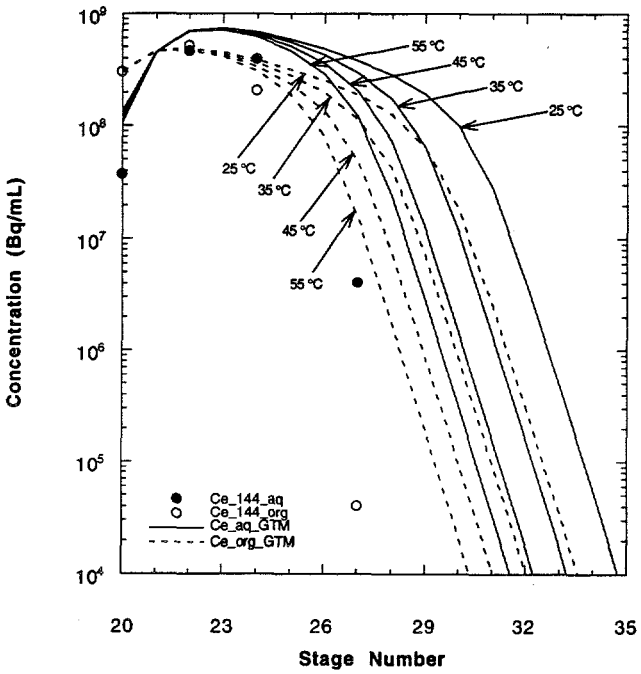

Fig. 28. Stagewise Aqueous and Organic Phase Concentration Profile for Cerium as a Function of Temperature for the Strip Section. Shown in this figure are the GTM simulations for 25°C, 35°C, 45°C, and 55°C at 90% stage efficiency for Run 2 and the experimental results obtained for this run.

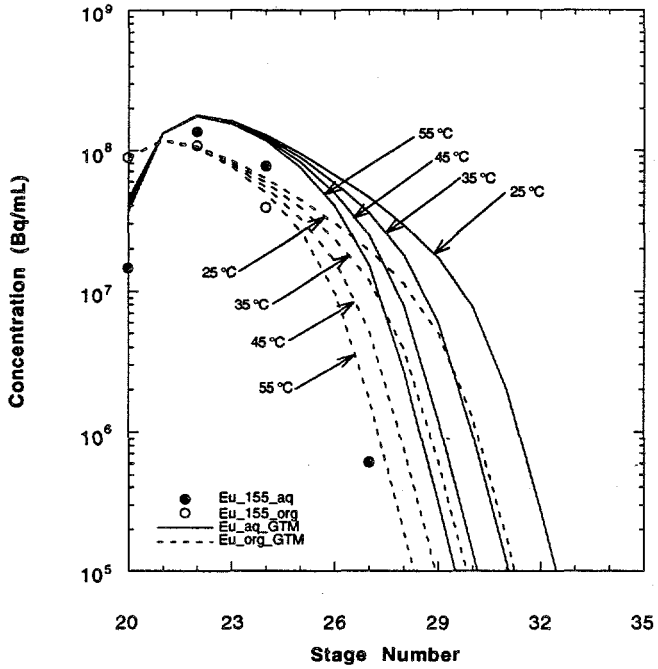

Fig. 29. Stagewise Aqueous and Organic Phase Concentration Profile for Europium as a Function of Temperature for the Strip Section. Shown in this figure are the GTM simulations for 25°C, 35°C, 45°C, and 55°C at 90% stage efficiency for Run 2 and the experimental results obtained for this run.

temperature is shown in Fig. 30. Similar results to those in Fig. 30 are obtained for curium and the rare earths. No temperature effects are seen for Cs and Ru since the GTM doesn't account for temperature dependence for these two components because the effects are too small.

Increasing the temperature has an adverse effect on the extraction section for Am, Cm, and the rare earths because it decreases their distribution ratios, thus increasing their concentrations in the aqueous phase. For the strip section, an increase in temperature also decreases the distribution ratio, but in this case a lower distribution ratio increases the effectiveness of the strip section, lowering the organic phase concentration that exits the strip section for the given components.

The effect of temperature on the plutonium distribution ratio is indirect. Although its effect on the distribution ratio for plutonium is too small to be included in the model that calculates the D value, a decrease in the distribution ratio for americium and the rare earths as the temperature increases will affect the concentration of plutonium in the aqueous phase. This indirect effect of temperature on the plutonium distribution coefficient can be seen in Fig. 31.

4. Equipment Type

Simulations using the GTM reported in the previous sections were generated by specifying a mixer-settler as the contacting equipment. Contact equipment type affects

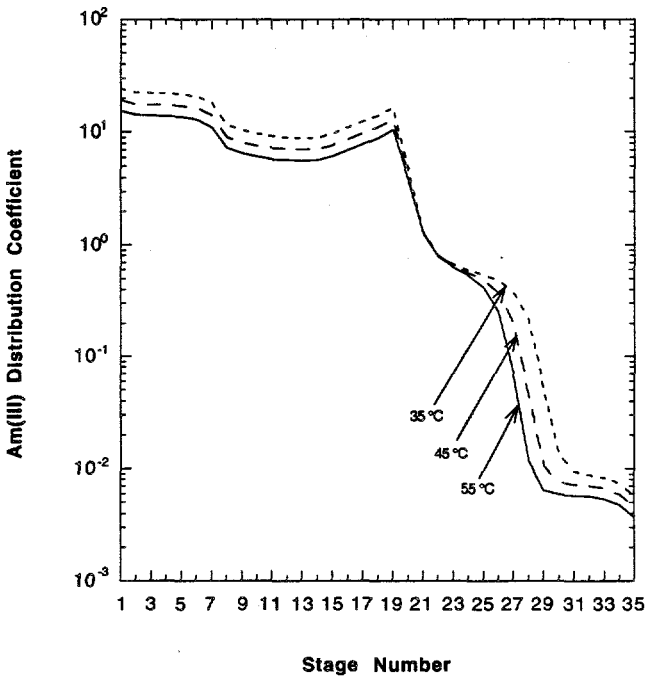

Fig. 30. Stagewise Distribution Coefficient Profile for Americium(III) in the Extraction/Scrub and Strip Sections as a Function of Temperature. Shown in this figure are the GTM simulations for 35°C, 45°C, and 55°C at 90% stage efficiency for Run 2.

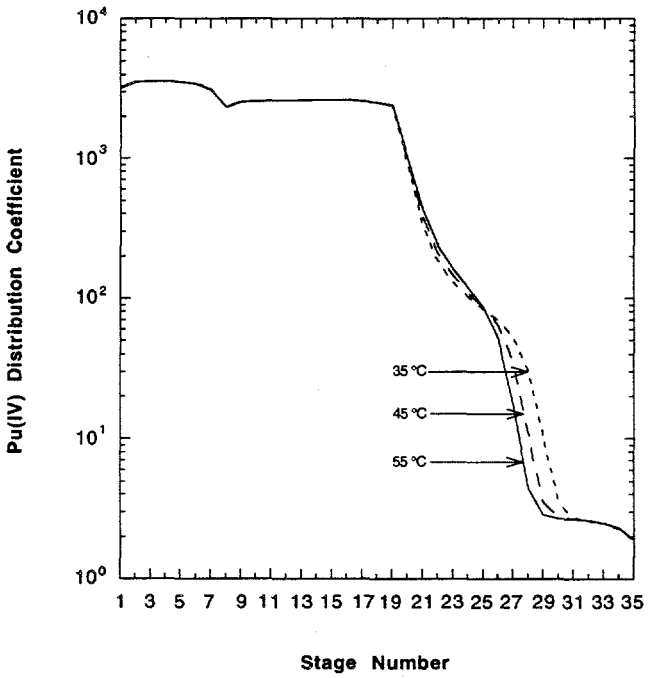

Fig. 31. Stagewise Distribution Coefficient Profile for Plutonium(IV) in the Extraction/Scrub and Strip Sections as a Function of Temperature. Shown in this figure are the GTM simulations for 35°C, 45°C, and 55°C at 90% stage efficiency for Run 2.

the way distribution coefficients are calculated in the GTM for Ru and Fe, since these components have a kinetic effect in their distribution ratio models. Iron was not present in the PNC feeds. In calculating the distribution ratio of ruthenium in a stage, the GTM takes into account the type of contact equipment used by assuming that the contact time is a matter of a few seconds (a centrifugal contactor) or a minute or more (pulsed columns and mixer-settlers). The difference in modeling these types of contacting equipment is that we assume that (1) in a pulsed column or mixer-settler, the contact time between the organic and aqueous phases is long enough that ruthenium species have time to equilibrate, and (2) in the centrifugal contactor, no reequilibration can occur, and the speciation that is present in the feed remains constant throughout the flowsheet.

In Figs. 32 and 33, we compare the concentration profile for ruthenium for Run 2 at 90% efficiency for both a mixer-settler and a centrifugal contactor. As in the case of temperature effects, all flowsheets were simulated using version 3.1 of the GTM, and, for consistency, 90% stage efficiency was used for all sections. Figure 32 shows the profiles for the extraction/scrub section, and Fig. 33 shows those for the strip section. These profiles imply that the distribution coefficient applied by the GTM for ruthenium should be lower for the extraction/scrub section and higher for the strip section.

C. Run 3

Analyses of the results reported for Run 3 are given only for the strip section, since those were the only results available in the literature [OZAWA-1992A]. The strip profiles produced by the GTM for this run are given in Figs. 34-39. For these figures, we have converted the molar concentration predicted by the GTM into units of becquerels per milliliter (as described at the beginning of Section IV) and plotted these concentrations versus the stage number for both aqueous and organic phases. Also given in these plots are the experimental concentration profiles reported by PNC. All flowsheets simulated for this run were done using version 3.1 of the GTM, and, for consistency, 90% stage efficiency, was used for all sections.

The operating conditions for PNC's Run 3 differ from those of Run 1 and Run 2. Run 1 and Run 2 were set up so that there was only a plutonium strip, whereas Run 3 was set up so that there were four strips: Am (stages 20-24), Np (stages 25-29), Pu (stages 30-34), and U (stages 35-39) (Table 1).

In Figs. 34 and 35, we show the concentration profiles obtained for Am and Pu using the GTM. As in the case of Run 2, the concentration profiles reported by PNC are given as a combination of ^{241}Am plus ^{238}Pu for one case (Fig. 34) and ^{239}Pu plus ^{240}Pu for the other case (Fig. 35). Since the ratio of these isotopes was not reported, it was not possible to report our GTM results as a combination. Instead, concentration profiles are given for Am(III) and Pu(IV) (Figs. 34 and 35, respectively).

Results for the americium strip can be seen in stages 20 to 24 in Figs. 34-39. The simulation results indicate that Am, Cm, Ce, Np, and Ru are all stripped in this section. The plutonium concentration in the organic phase is predicted to remain constant throughout this section. The predictions from the GTM are consistent with the PNC results except for ruthenium. As in Run 2, assuming a centrifugal contactor as the equipment type would improve the fit.

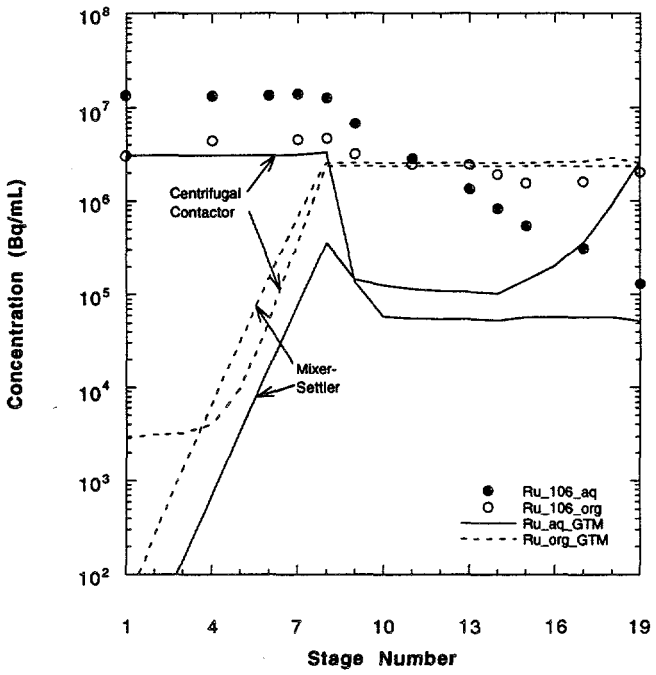

Fig. 32. Stagewise Aqueous and Organic Phase Concentration Profile for Ruthenium in the Extraction/Scrub Section for a Mixer-Settler and a Centrifugal Contactor. Shown in this figure are the GTM simulations for a mixer-settler and a centrifugal contactor at 90% stage efficiency for Run 2 and the experimental results obtained for this run.

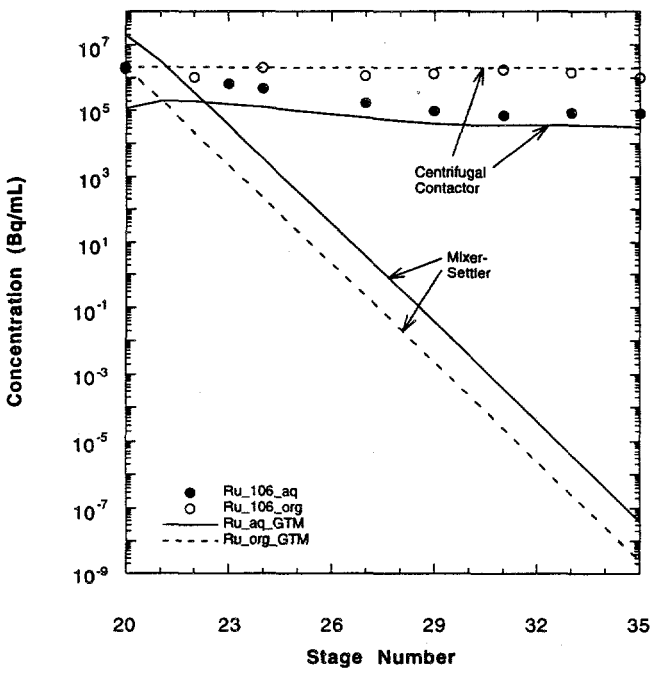

Fig. 33. Stagewise Aqueous and Organic Phase Concentration Profile for Ruthenium in the Strip Section for a Mixer-Settler and a Centrifugal Contactor. Shown in this figure are the GTM simulations for a mixer-settler and a centrifugal contactor at 90% stage efficiency for Run 2 and the experimental results obtained for this run.

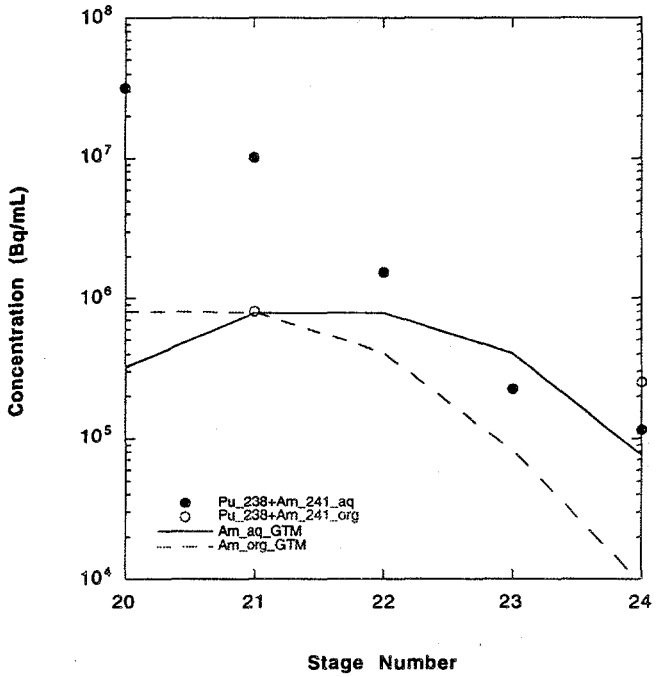

Fig. 34. Stagewise Aqueous and Organic Phase Concentration Profile for Americium in the Strip Section. Shown are the americium(III) results from the GTM simulation for the americium strip at 90% stage efficiency for Run 3 and the experimental results obtained for ^{241}Am plus ^{238}Pu for this run.

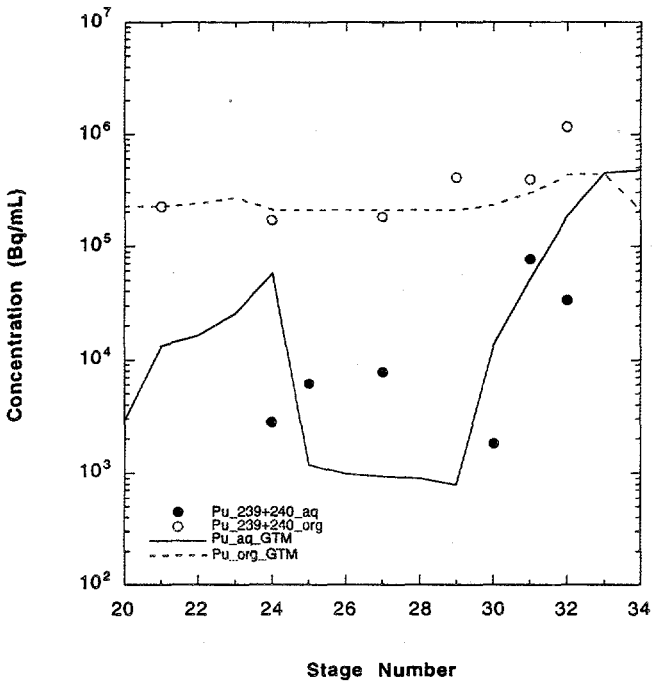

Fig. 35. Stagewise Aqueous and Organic Phase Concentration Profile for Plutonium in the Strip Section. Shown are the plutonium(IV) results from the GTM simulation for the Am, Np, and Pu strips at 90% stage efficiency for Run 3 and the experimental results obtained for ^{239}Pu plus ^{240}Pu for this run.

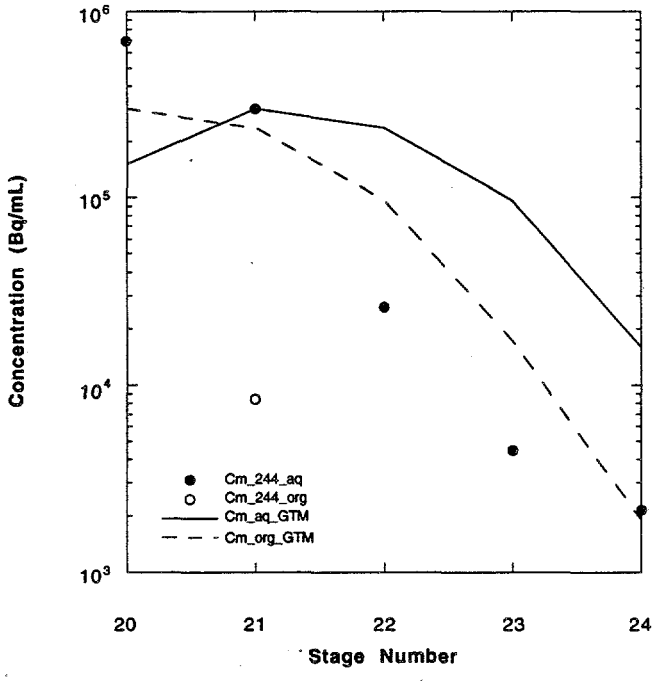

Fig. 36. Stagewise Aqueous and Organic Phase Concentration Profile for Curium in the Strip Section. Shown are the GTM simulation for the americium strip at 90% stage efficiency for Run 3 and the experimental results obtained for this run.

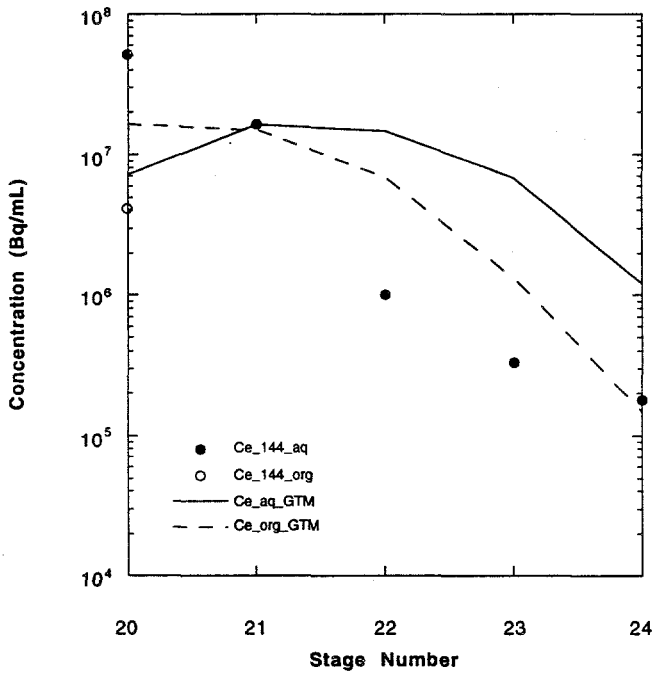

Fig. 37. Stagewise Aqueous and Organic Phase Concentration Profile for Cerium in the Strip Section. Shown are the GTM simulation for the americium strip at 90% stage efficiency for Run 3 and the experimental results obtained for this run.

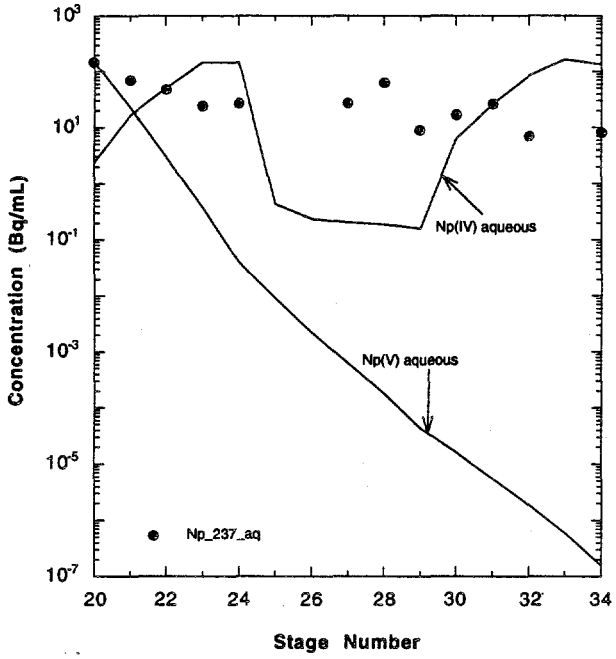

Fig. 38. Stagewise Aqueous Phase Concentration Profile for Neptunium(IV) and (V) in the Am, Np, and Pu Strip Section. Shown are the GTM simulation for 90% stage efficiency for Run 3 and the experimental results obtained for this run.

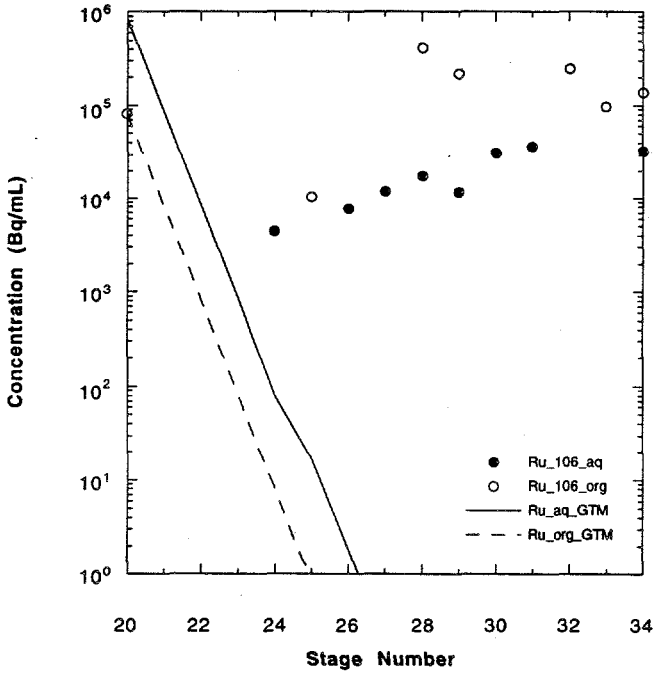

Fig. 39. Stagewise Aqueous and Organic Phase Concentration Profile for Ruthenium in the Am, Np, and Pu Strip Section. Shown are the GTM simulation for 90% stage efficiency for Run 3 and the experimental results obtained for this run.

Results for the neptunium strip can be seen in stages 25 to 29 and for the plutonium strip in stages 30 to 34 in Figs. 35, 38, and 39. For the neptunium strip, 0.1M HAN (hydroxyammoniumnitrate) was added to the feed for Np(V) to be reduced to Np(IV) and Pu(IV) to be reduced to Pu(III). An aqueous phase profile for both Np(IV) and Np(V) is given in Fig. 38. For Pu(III), a profile similar to that of Am(III) (Fig. 34) was obtained. The GTM's predictions indicate that Np(IV) will not be stripped in the neptunium strip and Pu(III) will not be stripped in the plutonium strip, under the given design conditions (Figs. 34 and 38).

REFERENCES

BATTLES

J. E. Battles et al., *Chemical Technology Division Annual Technical Report 1993*, Argonne National Laboratory Report ANL-94/15 (1994), pp. 76-77.

FELKER

L. K. Felker and D. E. Benker, *Application of the TRUEX Process to Highly Irradiated Targets*, Oak Ridge National Laboratory Report ORNL/TM-12784 (March 1995).

OZAWA-1992A

M. Ozawa, S. Nemoto, K. Nomura, Y. Koma, A. Togashi, "Some Modifications of the TRUEX Flowsheet for Partitioning of Actinide Elements in High Level Liquid Waste," Presentation for Organization for Economic Co-Operation and Development/Nuclear Energy Agency Meeting, "International Information Exchange Program on Actinide and Fission Product Separation and Transmutation," Argonne National Laboratory, November 11-13, 1992.

OZAWA-1992B

M. Ozawa, S. Nemoto, A. Togashi, T. Kawata, K. Onishi, "Partitioning of Actinides and Fission Products in Highly Active Raffinate from Purex Process by Mixer-Settlers," Solvent Extraction and Ion Exchange, **10**(5), 829-846, 1992.

OZAWA-1992C

M. Ozawa, S. Nemoto, T. Kawata, "Partitioning of Actinides Elements in High Level Liquid Waste with Bifunctional Extractant," Donen Giho, No. 82 (June 1992).

OZAWA-1993

Personal communication from M. Ozawa, PNC, to G. F. Vandegrift, Argonne National Laboratory, 1993.

VANDEGRIFT

G. F. Vandegrift et al., "Development and Demonstration of the TRUEX Solvent Extraction Process," Proceedings of the Symposium on Waste Management, Tucson, AZ, February 28-March 4, 1993, pp. 1045-1050.

Distribution for ANL-95/21

Internal:

B. D. Babcock
B. A. Buchholz
D. B. Chamberlain
L. Chen
M. K. Clemens
C. Conner
J. M. Copple
J. C. Cunnane
H. Diamond
D. Dong
D. W. Green
J. E. Harmon
J. E. Helt
E. P. Horwitz
J. C. Hutter
R. J. Jaskot
J. Laidler
R. A. Leonard
C. J. Mertz
L. Nunez
M. C. Regalbuto
J. Sedlet
W. B. Seefeldt
S. A. Slater
B. Srinivasan
M. J. Steindler
G. F. Vandegrift (20)
R. D. Wolson
D. G. Wygmans
TIS Files

External:

DOE-OSTI (2)
ANL-E Library (2)
ANL-W Library
Manager, Chicago Operations Office, DOE
A. Bindokas, DOE-CH
J. Haugen, DOE-CH
A. L. Taboas, DOE-CH/AAO
Chemical Technology Division Review Committee Members:
- E. R. Beaver, Monsanto Company, St. Louis, MO
- D. L. Douglas, Consultant, Bloomington, MN
- R. K. Genung, Oak Ridge National Laboratory, Oak Ridge, TN
- J. G. Kay, Drexel University, Philadelphia, PA
- G. R. St. Pierre, Ohio State University, Columbus, OH
- J. Stringer, Electric Power Research Institute, Palo Alto, CA
- J. B. Wagner, Arizona State University, Tempe, AZ

M. Dinehart, Los Alamos National Laboratory, Los Alamos, NM
C. W. Frank, USDOE, Office of Technology Development, Washington, DC
L. Holton, Pacific Northwest Laboratory, Richland, WA
S. C. T. Lien, USDOE, Office of Technology Development, Germantown, MD
G. J. Lumetta, Pacific Northwest Laboratory, Richland, WA
C. P. McGinnis, Oak Ridge National Laboratory, Oak Ridge, TN
A. C. Muscatello, LATO Office, Rocky Flats Plant, Golden, CO
A. L. Olson, Lockheed Idaho Technology Company, Idaho Falls, ID
M. Palmer, Los Alamos National Laboratory, Los Alamos, NM
G. Pfennigworth, Martin Marietta Energy Systems, Oak Ridge, TN
I. R. Tasker, Waste Policy Institute, Gaithersburg, MD
D. W. Tedder, Georgia Institute of Technology, Atlanta, GA
M. Thompson, Westinghouse Savannah River Company, Aiken, SC
T. A. Todd, Lockheed Idaho Techology Company, Idaho Falls, ID
S. Yarbro, Los Alamos National Laboratory, Los Alamos, NM